THE VIBRATIONAL RAMAN SPECTRA OF THE ν_1 SYMMETRIC MODE OF LIQUIDS METHANE AND CARBON TETRAFLUORIDE

RAJENDRA KUMAR JAIN


CENTRE FOR NFLD. STUDIES
JAN 26 1981
MEMORIAL UNIVERSITY
OF NEWFOUNDLAND

NOTICE

The quality of this microfiche is heavily dependent upon the quality of the original thesis submitted for microfilming. Every effort has been made to ensure the highest quality of reproduction possible.

If pages are missing, contact the university which granted the degree.

Some pages may have indistinct print especially if the original pages were typed with a poor typewriter ribbon or if the university sent us a poor photocopy.

Previously copyrighted materials (journal articles, published tests, etc.) are not filmed.

Reproduction in full or in part of this film is governed by the Canadian Copyright Act, R.S.C. 1970, c. C-30. Please read the authorization forms which accompany this thesis.

THIS DISSERTATION
HAS BEEN MICROFILMED
EXACTLY AS RECEIVED

AVIS

La qualité de cette microfiche dépend grandement de la qualité de la thèse soumise au microfilmage. Nous avons tout fait pour assurer une qualité supérieure de reproduction.

S'il manque des pages, veuillez communiquer avec l'université qui a conféré le grade.

La qualité d'impression de certaines pages peut laisser à désirer, surtout si les pages originales ont été dactylographiées à l'aide d'un ruban usé ou si l'université nous a fait parvenir une photocopie de mauvaise qualité.

Les documents qui font déjà l'objet d'un droit d'auteur (articles de revue, examens publiés, etc.) ne sont pas microfilmés.

La reproduction, même partielle, de ce microfilm est soumise à la Loi canadienne sur le droit d'auteur, SRC 1970, c. C-30. Veuillez prendre connaissance des formules d'autorisation qui accompagnent cette thèse.

LA THÈSE A ÉTÉ
MICROFILMÉE TELLE QUE
NOUS L'AVONS REÇUE

THE VIBRATIONAL RAMAN SPECTRA OF THE ν_1 SYMMETRIC MODE OF LIQUIDS METHANE AND CARBON TETRAFLUORIDE

by

Rajendra Kumar Jain (C)

A thesis submitted in partial fulfillment of the requirments
for the degree of Masters of Science.

Department of Physics
Memorial University of Newfoundland

July 1979

St. John's Newfoundland

ABSTRACT

The polarized or isotropic contributions to the totally symmetric (ν_1) vibrational Raman spectra of methane and carbon tetrafluoride were measured in the liquid phase along the liquid vapour co-existence line from the triple point to the critical point in each case. Attention was focussed on three principal characteristics of single component spectra; (1) the line width i.e. the full width at half maximum, (2) the shift in peak frequency relative to that at the triple point and (3) the degree of asymmetry observed in the line shape. Light from Ar^+ ion laser incident on the sample cell and scattered at 90^0 was analysed by a Fabry-Perot interferometer and recorded by photon counting systems. In case of methane, the line width remains practically constant from the triple point to the boiling point and increases from the boiling point onwards to the critical point, while in case of carbon tetrafluoride the line width is maximum at triple point and decreases up to the boiling point and afterwards remains constant up to the critical point. The observed variation in line width can be explained on the basis of a hydrodynamic theory of vibrational dephasing due to Hills and Madden. The relative Raman frequency shift has been found to vary linearly with density as previously observed in similar gas-phase experiments. In both the liquids the asymmetry in line shape is observed to be in opposite sense at the triple point to that at the critical point.

ACKNOWLEDGEMENTS

I express my sense of deep gratitude to Drs. M. J. Clouter and H. Kiefte for their guidance and valuable help at every stage of this work. I am also very much thankful to messers. S. F. Ahmad and N. Ali for some useful discussions. Thanks are also due to Mr. J. N. Prasad for his help in preparing this manuscript.

The excellent job of typing this thesis so efficiently in a very short time by Ms. Ruby Ryan is greatly appreciated.

Throughout this research work, I was supported by a Fellowship and a teaching assistantship from Memorial University of Newfoundland which I gratefully acknowledge.

Last but not the least, I am highly indebted to my father for his constant encouragement and support, without which this work would have been impossible

TABLE OF CONTENTS

CHAPTER - I

INTRODUCTION AND THEORY

1.0 Introduction

The molecular vibrational spectra of liquids have been studied for a long time using Raman scattering techniques. Interest has focussed primarily on the (anisotropic) contribution of the rotational degrees of freedom to a given band (i.e. the O and S branches), while the much sharper, purely vibrational contribution (the Q branch) has been largely neglected (Weber, 1973). In recent years, particularly with the advent of lasers, it has been possible to study the latter components in detail. The current interest in these components centers around the problem of understanding how the intermolecular interactions influence the shape (in particular, the width) of the Q branch profile. Given an adequate knowledge of the intermolecular pair-potential, as well as the various relaxation mechanisms involved, the pure vibrational Raman spectrum can be regarded as a relatively direct probe of the local environment in a fluid. This is of particular significance in the liquid phase where very few such experimental probes are known and where the behavior of the local environment is not well understood.

In this thesis it is demonstrated that a systematic investigation of the density and temperature dependence of the vibrational Raman spectrum in simple liquids can lead to significant information pertaining to the nature of the liquid state

1.1 Motional Narrowing

Among the mechanisms usually considered as being important in determining the shape of the Q-branch profile is one which is often referred

to as motional narrowing. However, for the particular liquids studied here it is concluded that this mechanism is only of minor importance. A brief presentation of the arguments leading to this conclusion will now be given. A Raman Q branch consists of a series of closely spaced lines encompassing the complete set of rotational states of the molecule. In most molecules the difference between B_{υ}' and B_{υ}'' (where B_{υ}' and B_{υ}'' are the rotational constants for the vibrational levels υ' and υ'') is so small that the lines of the Q branch cannot be resolved, except at very low density because of the normal pressure broading of these individual components.

When overlapping of the Q branch components occurs it has been found that the line starts to narrow as the density is further increased. This is called motional narrowing and is present because of the interaction between vibration and rotation. Alekseyev and Sobleman (1969) and later on Temkin and Burshtein (1976) have given a theoretical treatment of the effect and have shown that the full width at half maximum (FWHM) Γ is

$$\Gamma = 2(\rho\sigma_J V)^{-1}\left(\frac{\alpha_e}{B_e}\frac{kT}{\hbar}\right)^2 \qquad (1.1)$$

where ρ is the gas density, σ_J is the cross-section for the scattering with change of rotational state, V is the average thermal velocity, α_e is the vibration-rotation interaction constant, B_e is the equilibrium rotational constant, k is the Boltzmann constant and T is the temperature. From equation (1.1), it is evident that the width decreases as density increases. At very high densities the motional narrowing is complete and further broadening is caused by direct vibrational perturbations. The line width of liquid N_2 has been measured by Clouter and Kiefte (1977) from the triple point to the critical point. At 77 K they found the width to be 2 GHz. Brueck (1977) has calculated theoretically the line width contribution due to motional narrowing to be 0.99 GHz at 77K (boiling point of N_2), a significant

fraction of the total width of 2 GHz. Therefore, it is clear that motional narrowing can contribute to the line width up to very high densities in some liquids. On the other hand it appears that motional narrowing does not contribute significantly in the case of the totally symmetric ν_1 vibrational mode of liquid CH_4. The reason for this can be attributed to the value of α_e^2 (see Eq. 1.1). For N_2, α_e^2 is $(0.0187)^2$ cm^{-2} (Varghese, 1967) and for CH_4, α_e^2 is $(0.0034)^2$ cm^{-2} (Jones, 1972). That is, in methane the Q branch components are much more closely spaced than in N_2, so that the motional narrowing occurs at a much lower density. The line width of the ν_1 symmetric mode of CH_4 has been measured by Clements (1972) to be 9.6 GHz at a density of 2 Amagats in the gas phase. He found that as pressure is increased the width increases. This clearly indicates that motional narrowing is not significant for methane at the much higher densities involved in the present work and it will not be considered further.

1.2 Band Shape Analysis

In the band shape problem one, in principle, studies experimentally the response of a system to an external field which is weakly coupled to the system. Because the response of a system to a specific weak probe is directly related to a correlation function, various spectroscopic techniques can be applied to measure spatial and time dependent correlation functions. Raman spectroscopy is utilized to observe the dynamics of vibrational energy transfer in a liquid system via the vibrational correlation function. This correlation function is obtained by the Fourier transform of the isotropic component of vibrational Raman scattered light and describes contributions from (1) the loss of phase coherence, and, (2) population or energy relaxation involving the particular excited state. The mechanism of dephasing for a dilute gas is simpler than for a liquid. In a dilute gas, the vibrational wave function of a molecule can be described by its quantum state and an over all phase. The elastic collisions give rise to phase shifts and

the inelastic collisions to population relaxation. In a dilute gas, collisions can be assumed to be mainly binary and in a series of such collisions the phase will change by different amounts. This will depend upon the orientations, relative momenta and the impact parameters of the interacting molecules. The phase of the wavefunction will lose its correlation with its initial value after a sufficient number of elastic collisions. Thus for an ensemble of molecules the phase of the wave functions will have a random distribution of values between 0 and 2π. This is called phase relaxation, or dephasing.

In a liquid, a given molecule interacts continuously with many neighbours, hence the description of vibrational relaxation is quite complicated. Bratos and Marechal (1971) have described the dephasing in a liquid in the following way. The environment causes a slight perturbation of the excited oscillator, causing it to vibrate at a slightly different frequency. The perturbations, however, are assumed to be too small to induce a significant number of transitions between vibrational levels. As a result the correlation function $\langle q(o)\, q(t)\rangle$ describes the rate at which the ensemble of oscillators loses phase coherence, where q is the vibrational coordinate. With respect to population relaxation one normally considers the transfer of vibrational energy to external degrees of freedom (translational and/or rotational). In case of the near resonance condition, the energy could also be transferred to another fundamental mode of the collision partner. In addition, the process of resonant transfer of energy from one vibrationally excited molecule to the same vibrational mode of a neighbouring molecule must be mentioned, but is normally treated as a part of the dephasing process. Though all these processes may occur, the individual process or processes depend upon the particular molecular system.

As pointed out above vibrational relaxation consist of the processes of (i) energy relaxation and (ii) phase relaxation. In conventional Raman spectroscopy it is not possible to separate out these processes, i.e., to measure the energy relaxation time τ_1 and dephasing time τ_2. However, they can be measured separately using pico-second pulsed laser techniques. A detailed review article by Laubereau and Kaiser (1978) gives the experimental and theoretical results for a number of molecules. It has been found that usually $\tau_1 >> \tau_2$ so that the line widths in vibrational spectra are mainly determined by τ_2, the dephasing time. For instance in the liquid N_2 (at 77K) τ_2 is ~ 75 pS and τ_1 ~ 1S. However, τ_2 and τ_1 are comparable for many organic liquids. In these cases intramolecular processes may provide alternative and more efficient routes for dissipating the vibrational energy. An example of this type of energy transfer can be seen from the study of the binary mixture of CH_3CCl_3 and CD_3OD by Laubereau et al. (1973). The measured τ_1 and τ_2 for the symmetric CH_3 stretching vibration at 2939 cm^{-1} was found to be 5 pS and 1 pS respectively. These authors showed that a quantum of energy from the CH_3 vibration decays into a C-D vibration at 2227 cm^{-1} with the residual energy being taken up in a C-Cl vibration at 713 cm^{-1}.

To study the molecular motions, it is necessary to know how the dipole moment $\vec{P}$ and polarizability $\tilde{\alpha}$ respond to changes in the vibrational, orientational and translational coordinates of a molecule and also to changes in the coordinates of surrounding molecules. Intermolecular interactions also cause fluctuations in $\vec{P}$ and $\tilde{\alpha}$ and their induced effects determine some features of the correlation functions.

In Raman scattering experiments, broadening of the line shape due to rotation contributes differently to the polarized and depolarized Raman band components. This allows a means for separating the reorientational from the non-reorientational processes contributing to the band shape. It is well known that the depolarized vibrational Raman scattering intensity is determined by the anisotropy of the polarizability derivative tensor, while the polarized scattering results from contributions due to both isotropic and anisotropic components.

Nafie and Peticolas (1972) assumed that the vibrational relaxation is the major non-reorientational broadening mechanism and derived the expressions for depolarized and polarized components of the vibrational Raman scattered light. Their theory is outlined below. Gordon (1965) has shown that the intensity of scattered radiation for an isolated oriented molecule is given by

$$I(\omega) = A(\omega_I - \Omega_\nu)^4 \sum_a \rho_a \sum_b \sum_i \rho_i \sum_f |\langle i|\hat{\varepsilon}_I \underset{\sim}{\alpha}^\nu \hat{\varepsilon}_s|f\rangle \times (\phi_b^\nu|Q^\nu|\phi_a^\nu)|^2 \, \delta(\omega + \omega_f - \omega_i) \tag{1.2}$$

where A is a constant of proportionality, ω_I and Ω_ν are the frequencies associated with the incident light and the ν^{th} normal mode of vibration respectively. $\hat{\varepsilon}_I$ and $\hat{\varepsilon}_s$ are the polarization directions of the incident and scattered light and $\underset{\sim}{\alpha}$ is the polarizability tensor of the medium, i and f label the initial and final states of the system, ρ_i is the Boltzmann factor governing the population of the initial states and $|\phi_a^\nu\rangle$ and $|\phi_b^\nu\rangle$ are the eigen-kets of the initial and final ground state

vibrational wave functions.

Nafie and Peticolas (1972) introduced an additional term describing intramolecular and intermolecular vibrational relaxation, as well as random vibrational frequency fluctuations. This accounts for the principal broadening mechanism for Raman line shapes when the effects of reorientation have either been separated or are not present. Converting equation (1.2) from Schrodinger picture to Heisenberg picture they showed that

$$I_{iso}(\omega) = I_{VV}(\omega) - \frac{4}{3} I_{VH}(\omega) \tag{1.3}$$

$$\text{and } I_{aniso} = I_{VH}$$

where I_{VV} and I_{VH} can be expressed as

$$I_{VH} = \frac{A(\omega_1 - \Omega_\nu)^4}{2\pi} \int_{-\infty}^{\infty} < \frac{1}{10} \mathrm{Tr}\,[\underset{\approx}{\beta}^\nu(0)\ \underset{\approx}{\beta}^\nu(t)]>_{tr} \times \tag{1.4}$$

$$<Q^\nu(0)Q^\nu(t)>_{vib} \exp i\omega t\, dt,$$

$$I_{VV} = \frac{A(\omega_1 - \Omega_\nu)^4}{2\pi} \int_{-\infty}^{\infty} <(\alpha^\nu)^2 + \frac{2}{15} \mathrm{Tr}[(\underset{\approx}{\beta}^\nu(0).\underset{\approx}{\beta}^\nu(t)]>_{tr} \times \tag{1.5}$$

$$<Q^\nu(0)\, Q^\nu(t)>_{vib} e^{i\omega t}\, dt$$

The terms α^ν and $\underset{\approx}{\beta}^\nu$ correspond to the division of the polarizability $\underset{\approx}{\alpha}$ into its average

$$\alpha^\nu = \frac{1}{3} \mathrm{Tr}\ \underset{\approx}{\alpha}. \tag{1.6}$$

and its traceless anisotropy

$$\underset{\sim}{\beta}^{\nu} = \underset{\sim}{\alpha} - \alpha \underset{\sim}{I} \tag{1.7}$$

The term $\langle Tr[\beta(o) \cdot \beta(t)]\rangle$ is the rotational translation correlation function and the term $\langle Q^{\nu}(o)\, Q(t)^{\nu}\rangle_{vib}$ is the vibrational correlation function. In $I_{VV}(\omega)$ and $I_{VH}(\omega)$, V and H represent the vertical and horizontal directions of polarization.

Using equation (1.4) and (1.5) one obtains

$$I_{iso}(\omega) \equiv \frac{I_{VV}(\omega) - \frac{4}{3} I_{VH}(\omega)}{\int_{-\infty}^{\infty} [I_{VV}(\omega) - \frac{4}{3} I_{VH}(\omega)]d\omega}$$

$$= \frac{1}{2\pi} \int_{-\infty}^{\infty} \langle Q^{\nu}(o)\, Q^{\nu}(t)\rangle_{vib}\, e^{i\omega t}\, dt \tag{1.8}$$

and the vibrational correlation function can be expressed as

$$C_v(t) = \langle Q^{\nu}(o)\, Q^{\nu}(t)\rangle = \int_{-\infty}^{\infty} I_{iso}(\omega) e^{-i\omega t}\, dt \tag{1.9}$$

Kubo (1961) has developed a stochastic theory of line shapes and relaxation phenomena. He considered the motion of an oscillator and showed that the amplitude of modulation Δ can be expressed as

$$\Delta^2 = \int \omega_1^2\, P(\omega_1) d\omega_1 = \langle \omega_1 \rangle^2 \tag{1.10}$$

and $$\omega(t) = \omega_0 + \omega_1(t) \tag{1.11}$$

where $\omega_1(t)$ represents the fluctuations in the frequency, the average of which is zero

$$\text{i.e. } \bar{\omega}_1 = 0 \tag{1.12}$$

Kubo (1961) defined the correlation function of modulations as

$$\psi(t) = \frac{1}{\Delta^2} \cdot < \omega_1(t)\omega_1(t+\tau) > \ , \tag{1.13}$$

then the correlation time τ_c is given by

$$\tau_c = \int_0^\infty \psi(t)dt \ . \tag{1.14}$$

It was shown that when $\Delta.\tau_c << 1$, this is the condition for fast modulation and in the limit $\Delta.\tau_c \to 0$, the line approaches a Lorentzian form in which the half-width $\Gamma = \Delta^2\tau_c$ and when $\Delta.\tau_c >> 1$, the line shape is Gaussian.

The corresponding expressions for Lorentzian and Gaussian shapes respectively, are as follows

$$I(\omega-\omega_o) = \frac{1}{\pi} \frac{\Gamma}{(\omega-\omega_o)^2 + \Gamma^2} \tag{1.15}$$

and

$$I(\omega-\omega_o) = \frac{1}{\sqrt{2}\pi\ \Delta} \exp\{-\frac{(\omega-\omega_o)^2}{2\Delta^2}\} \tag{1.16}$$

Rothschild (1976) considered the vibrational resonance energy transfer and dephasing in liquid N_2 and has shown that the Kubo correlation function can be written (in case of fast modulation) as

$$\psi(t) = \exp[\{-<\{\omega_1(o)\}^2> [\tau_c^2(\exp(-t/\tau_c)-1) + t\ \tau_c]\}] \tag{1.17}$$

The quantity $\langle \omega_1(o)^2 \rangle$ is identified with the second vibrational moment i.e. $\langle \{\omega_1(o)^2\} \rangle^{1/2} = (M_2(v))^{1/2}$ where the second spectral moment of the isotropic band shape is given by (Kubo, 1961).

$$M_2(v) = \frac{\int_{-\infty}^{\infty} I_{iso}(\omega)\ [\omega-\omega_o]^2\ d\omega}{\int_{-\infty}^{\infty} I_{iso}(\omega)\ d\omega} \qquad (1.18)$$

Taking the Fourier transform of equation (1.17), one obtains

$$I_{iso}(\omega) = \frac{I_{max}}{[1 + \omega^2\ \tau_c^2][1 + \omega^2\ \tau_v^2]} \qquad (1.19)$$

where $\tau_v \simeq \frac{1}{M_2(v)\tau_c}$, ω is the angular frequency displacement from the band centre and τ_v is the vibrational relaxation time. By measuring the $I_{iso}(\omega)$, it is possible to determine vibrational and Kubo correlation times (τ_c), to decide whether the line shape is Lorentzian or Gaussian [Rothschild, 1976]. However, in the present work, because of the experimental difficulties, this was not possible.

The isotropic Raman line widths have been measured for a number of molecules. Most of the workers studied these molecules mainly to separate vibrational relaxation from rotational relaxation. As far as is known to the present author, except for Clouter and Kiefte (1977), no measurements for the isotropic line widths of the Raman Q branch from the triple point to the critical point have been made. A survey of all the molecules studied so far has been made by Oxtoby (1979). It is important to study

line widths in the entire range from the triple point to the critical point since the various molecules behave quite differently over this range. There is no complete theory available for the change in line width from triple point to boiling point, neither is there a comprehensive theory found in the literature for the observed critical anomaly. The main purpose of this work is to study how the line width varies with temperature in case of saturated liquid CH_4 and CF_4 and to comment on aspects of the theory. These molecules are theoretically simple since they belong to the spherically symmetric T_d group.

1.2 Critical Phenomena

Since this thesis mainly describes the critical anomaly, a brief introduction of critical phenomena would not be out of place. Critical phenomena are caused by a balancing out of the effects of short-range intermolecular repulsion and very long range attraction. The critical temperature is determined by the condition that $\frac{\partial p}{\partial v}$ and $\frac{\partial^2 p}{\partial v^2}$ both vanish. The phase below the critical point is an ordered phase. It can be characterised by an order parameter that goes to zero at the critical point. The response function of the order parameter diverges at the critical point, which indicates that the system has reached a limit of stability. In fluids the order parameter is the density difference from critical density $\rho - \rho_c$, its response function is the derivative of density with respect to pressure. It has been tried to explain critical phenomena with the help of critical exponents. Guggenheim (1945) plotted reduced density (ρ/ρ_c) vs. T/T_c for eight fluids. Fits to an equation $(\rho - \rho_c) \sim (-\epsilon)^\beta$, where $\beta = \frac{1}{3}$ and $\epsilon = \frac{T - T_c}{T_c}$

were found. Since then β has been measured experimentally by a large number of authors. It appears to have a value of ~0.34 for fluids. The other common critical exponents γ and γ', are defined by

$$\frac{K_T}{K_T^o} \propto \begin{cases} (-\varepsilon)^{-\gamma'} & [T < T_c] \\ (\varepsilon)^{-\gamma} & [T > T_c] \end{cases} \qquad (1.20)$$

where K_T is isothermal compressibility and $K_T^o = \frac{1}{p_c^o} \equiv \frac{m}{kT_c\rho_c}$, which is the compressibility of an ideal gas of density ρ_c at $T = T_c$. Stanley (1971) has described, in detail, all the critical exponents and has discussed their theoretical and experimental values.

By virtue of the divergence of K_T at the critical point the low angle scattering becomes very large as the critical point is approached in the one phase region. This anomalous critical scattering with visible light is known as critical opalescence. Physically it can be understood as follows: As the compressibility becomes large, long-wavelength density fluctuations are allowed to grow to large amplitude. Formation and disruption of 'flickering' clusters of $\sim 10^3$-10^4 molecules from the locus of equilibrium separation takes place. These clusters are of such a dimension that they may scatter at optical wavelengths. This is seen by the appearence of the typical milky colour. A way of describing these phenomena is by means of the correlation function G(r), which measures the extent to which the local particle densities, a distance r apart, are correlated. Ordinarily the range of G(r) is the correlation length ξ (Orestein-Zernike length). Below the critical temperature ξ is of the order of the range of the interaction between the particles. Near the critical point ξ diverges and the Fourier

transform of G(r), the structure factor S(Q), governs the scattering power of the medium. At the critical point S(Q) diverges for small wavenumbers Q.

1.3 Recent Theoretical Studies

In a series of papers Hills (1978 a, b) and Hills and Madden (1979) have developed a theory of vibrational relaxation in liquids. They used a continuum description of the fluid surrounding a vibrationally excited molecule. It was shown that the vibrationally excited probe molecule relaxes through interactions with the density fluctuations in the surrounding solvent fluid. The interaction occurs through a potential $V_L(Q)$. The range of $V_L(Q)$ determines which Q-fourier components of the density fluctuations are most effective in causing vibrational relaxation. These authors obtained expressions for the dephasing time and also for the energy relaxation time in terms of the dynamical structure factor $S(Q, \omega)$. A further discussion of this theory is given in chapter III.

1.4 Thesis Outline

The second chapter of this thesis deals with the experimental apparatus and technique. In this chapter the apparatus has been briefly described, as it has been described in a number of other theses from this department.

Chapter III consists of the results and discussion. Two liquids namely methane and carbon tetrafluoride were studied. Their isotropic vibrational Raman line widths and frequency shifts were obtained using the apparatus described in chapter II. An attempt has been made to explain the observed line widths from the boiling point to the critical point using the theory of Hills and Madden (1979). The relative frequency shift has also been explained on the basis of theory proposed for gas phase. It has not been possible to explain the line width at and near the triple point as no

theory is available for this phenomena in the literature. It is not unlikely, however, that this effect is associated with the onset of short range orientational order.

CHAPTER - II

EXPERIMENTAL APPARATUS AND TECHNIQUE

2.0 Experimental Apparatus

The work in this thesis involves measurements of Raman spectra of saturated liquids as a function of temperature. In order to carry out the measurements, the source of incident radiation used was an Argon-ion laser (Model 165-08, Spectra Physics), which was focussed at the centre of a temperature controlled high pressure cell containing the liquid sample. The light scattered at 90^{o} was passed through a grating monochromator and was analysed by a Fabry-Perot interferometer, followed by a photon counting system.

The photon counting system consists of a cooled ITT FW 130 Photomultiplier tube as a basic detector followed by an amplifier/ discriminator (Princeton Applied Research Model SSR 1120) and a Data Acquisition and Stabilization system (Burleigh Model DAS-1). The overall arrangement of the apparatus used is shown schematically in Fig. 2.1. The experimental set-up has been described in more detail in a number of theses (Morgan, 1976; Ahmad, 1977; Gammon, 1978; and Ali, 1978) from this department. Therefore only a brief account of the set-up will be given here.

A2.1 Laser

The Argon ion laser, used in this work, has a good stability and a narrow line width in its output frequency. The average width of the laser

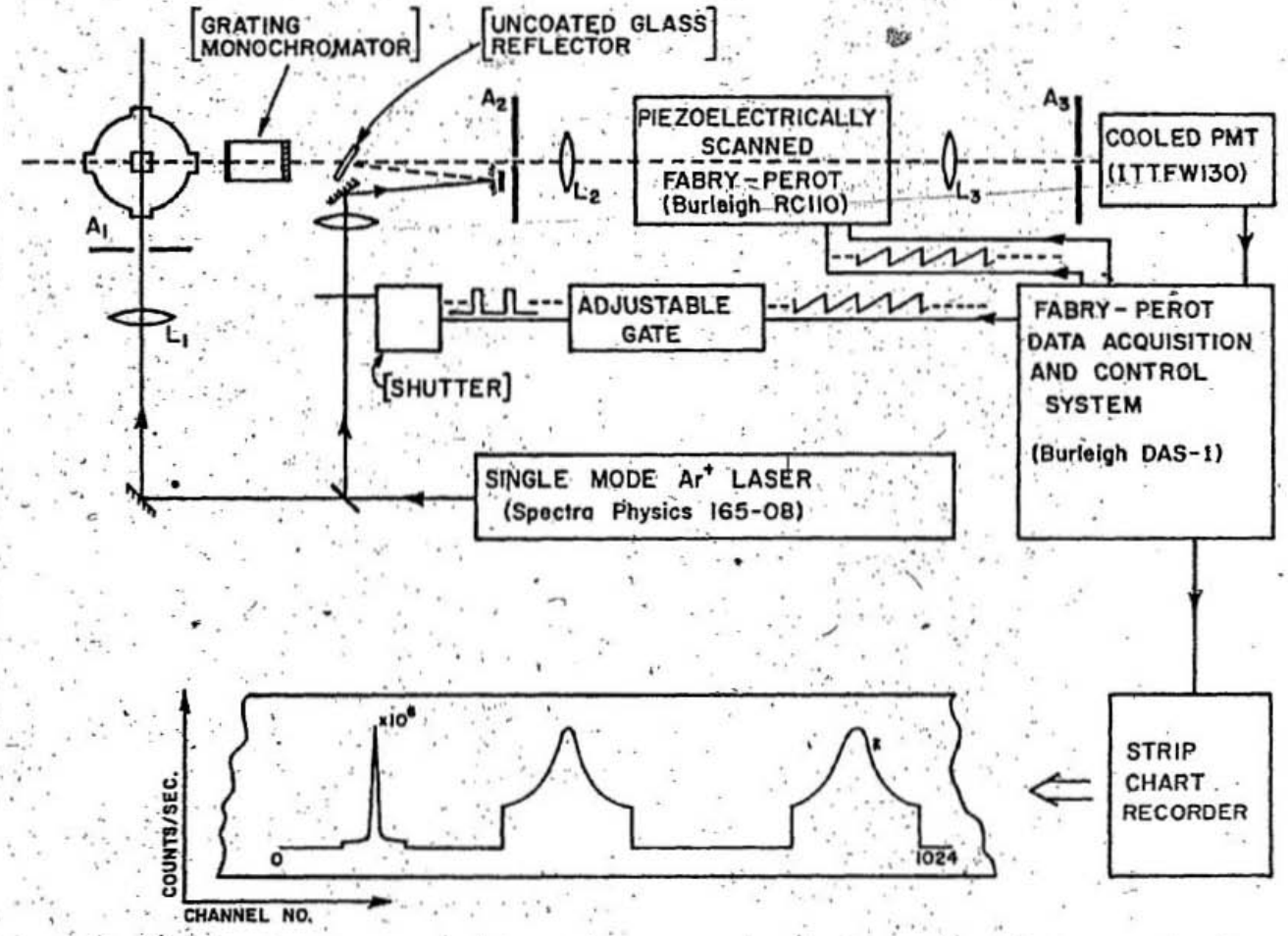
GRATING MONOCHROMATOR
UNCOATED GLASS REFLECTOR
A1
A2
A3
L1
L2
L3
PIEZOELECTRICALLY SCANNED FABRY-PEROT (Burleigh RC110)
COOLED PMT (ITTFW130)
ADJUSTABLE GATE
[SHUTTER]
FABRY-PEROT DATA ACQUISITION AND CONTROL SYSTEM (Burleigh DAS-1)
SINGLE MODE Ar+ LASER (Spectra Physics 165-08)
STRIP CHART RECORDER
x10^6
0
1024
COUNTS/SEC.
CHANNEL NO.

Fig. 2.I

line due to high frequency 'jitter' was found to be about ±5MHz. This laser essentially consists of a gas discharge tube, excited with a direct current of about 25A and is placed in an optical cavity of length 1.18m. A prism in the laser cavity was angled so as to limit the lasing to the 514.5 nm line in the Ar^+ spectrum. The laser action of this line was confined to one mode by using a temperature controlled intercavity etalon assembly. It was found that 'mode hopping' vanishes after warming up of a few hours. The beam from the laser was directed by way of a beam steerer and a lens at the centre of the sample cell.

2.1 The Liquid Cell

The cell used in the present work is quite suitable for studying either a gas or liquid sample. It can withstand large temperature and pressure variations. It has been described fully in the thesis of Morgan (1976) and by Clouter et al. (1975). In the beginning of the experiment, the cell was found to be dirty and leaking. Therefore it was taken apart for cleaning and for removal of the leaks. The cell is quite small (a cube $\simeq (2.5)^3$ cm^3) in dimensions. It was necessary for it to be of small size in order to avoid i) the effects of differential thermal expansion between dissimilar materials involved and ii) to minimise thermal gradients. It is made up of BeCu alloy in the shape of a cube. The scattering volume was located at the intersection of three mutually perpendicular holes, two horizontal and one vertical. The holes were closed by quartz plates. The four quartz plates were glued (using silicone rubber cement) to four metal plates. These metal plates were sealed with an indium O-ring seal to the cell (Clouter et al. 1975). Considerable care was required in sealing the windows, to avoid the

development of leaks. After cleaning and rinsing throughly in acetone and spectroscopic methanol, the cell was assembled and it was found that there was no leak in the cell up to 1000 psi.

The cell inlet tube was hard soldered into the top of the cell. This inlet tube was externally connected to the gas tank as well as a series of three Bourdon-tube gauges and a rupture-disc pressure fuse. A tube of smaller diameter than the inlet tube was inserted into the inlet tube. This was done to reduce the volume of the gas. The inlet tube entered the cryostat at the top through a vacuum O-ring seal. It was found that the cell did not stay permanently at any fixed position. Due to temperature and pressure changes it could go either up or down or even rotate. To overcome this problem a suitable clamp was designed and the cell was fastened properly so that it remained stable and fixed.

A platinum resistance thermometer was mounted on the cell as close as possible to the scattering site to determine the temperature of the sample. To cool the cell, thermal contact between the cell and the cryostat was made by two copper braids which were soft soldered to the two posts at the top of the cell, and extended upwards to a heat sink at the bottom end of a heat exchange column. An electrical heater of resistance 60 Ω was wound on these two posts. The heater was used in conjunction with a Ga As thermometer to automatically control the temperature of the cell.

2.2 Cryostat

A schematic diagram of the sample cell and cryostat is shown in Fig 2.2. It is described with the help of diagram as follows. The gas inlet

Figure 2.2

1. Electrical feedthrough
2. Exchange gas port
3. Nitrogen fill and vent
4. Nitrogen vent
5. Nitrogen fill
6. Nitrogen reservoir (outer)
7. Exchange gas chamber
8. Vacuum gap
9. Sample support tube
10. Nitrogen reservoir (inner)
11. Outer tail section
12. Nitrogen temperature radiation shield
13. Heat sink
14. Sample cell
15. Quartz window
16. Copper braids
17. Clamp

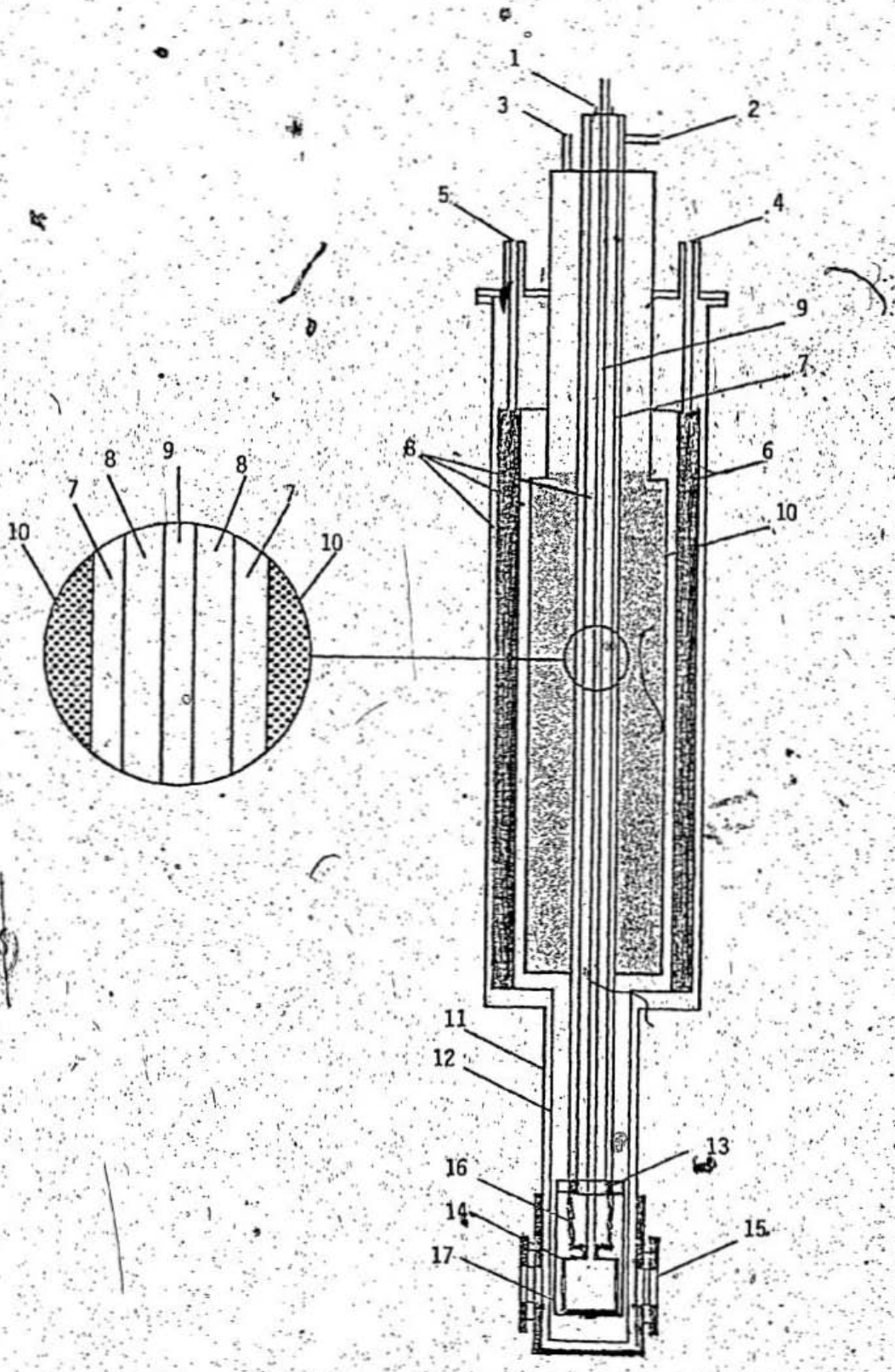

FIGURE 2.5

tube, which is connected to the scattering cell was surrounded by an annular exchange gas chamber (7) and was insulated from it by a vacuum space (8). A relatively large brass ring (13) was used to close the bottom of exchange gas column. This ring also served the purpose of heat sink. The gas exchange chamber was surrounded by two concentric coolant reservoirs, the inner one meant for use with liquid helium and the outer with liquid N_2. Liquid helium was necessary only to get temperature below 80 K, otherwise the inner cylinder was filled with liquid nitrogen and the other was evacuated in the temperature region from 90 K upwards. The two reservoirs were also separated from each other by a vacuum space (8). The outer reservoir (6) was also insulated from the outerside environment by a vacuum space between it and the outer shell of the cryostat. A tube (not shown in the Figure) with a heater wound around it also surrounded the gas inlet tube. Because of the temperature gradient between the upper and lower portion of this tube, it was found that gas would condense in the lower portion and drop into the cell. By switching the heater on, the sample remained as gas inside the lower portion of the gas inlet tube. The scattering cell was suspended in the tail section of the cryostat. The internal volume of the cryostat was evacuated to 10^{-5} torr, and the liquid coolant reservoir was filled with liquid nitrogen. The exchange gas was either N_2 or O_2. It was found that up to 140 K, O_2 was a better exchange gas, but for temperatures above 140 K, N_2 was more suitable. The exchange gas provided the necessary thermal link between the liquid coolant and the sample site via the heat sink. The gas in the exchange gas chamber condenses near the cold wall of the liquid N_2 reservoir (10) and falls to the heat sink (13) to which the cooling braids of the cell were connected. The sink temperature is then reduced on evaporation of the condensed exchange gas. A crude control could

be made by varying the amount of exchange gas.

The complete cryostat with the scattering cell (18) was vertically suspended on a metal frame.

2.3 Interferometer

For different samples, the vibrational Raman frequencies are different. Hence for every sample one needs to have a filter passing only the Raman vibration frequency of that sample. In order to avoid keeping a large set of expensive fixed filters, a variable filter is desirable. Therefore a grating monochromator (Bausch and Lomb, 500 mm) was used. The reflection grating had a 600 groves/mm and dispersion sufficient to limit the pass band to ~ 2.5 nm, when using slit widths of 1 mm. The transmission efficiency, with the polarization direction parallel to the grating rulings was ~ 60%.

The light scattered at 90^{o} was analysed by a Burleigh Model RC-10 Fabry-Perot interferometer. The theory and the performance of the interferometer have been discussed by various authors, for example Jenkins and White (1957), Jones (1972), etc. Basically the FP Interferometer consists of two high precision, reflecting optical plates separated by a distance 'd' and held parallel to each other. The equation describing the condition for constructive interference in a FP interferometer is as follows:

$$N\lambda = 2dn \cos \theta \qquad (2.1)$$

Here N is the order number, λ is the wavelength of light, n is the refractive index of the medium between the plates and θ is the angle the incident ray makes with interferometer axis. However, only the light transmitted along the optic axis for which $\theta \simeq 0$ was studied, known as central spot scanning. Equation (2.1) becomes for $n = 1$ in the air

$$N\lambda = 2d \tag{2.2}$$

The order number and transmitted wavelength could be changed by varying the spacing (d). To observe a spectrum the scanning was done by making small continuous variation in the plate separation with the aid of three piezoelectric stacks arranged in a triangular pattern behind the rear reflector. The plate separation (d) varied linearly(to a good approximation) with the applied voltage to the piezo-electric elements. Proper alignment was a critical factor in maximising the resolution and peak transmission from the interferometer. Rough adjustment in plate separation and alignment could be done mechanically. For finer adjustments a separate voltage to each individual element was applied to control the orientation of the rear/FP plate; this voltage was provided by the DAS. The DAS also automatically controlled the the FP interferometer alignment.

The free spectral range (FSR) can be defined as the frequency interval between the two consecutive orders of the FP interferometer. Thus

$$FSR = \frac{c}{2d} \quad \text{(in Hz)} \tag{2.3}$$

where c is the velocity of light in vacuum. All frequency shifts and widths

measured in this experiment were determined relative to the FSR. The plate separation was obtained using a micrometer screw mechanism to move a ball bearing back and forth ten times between the plates. This ball bearing was connected to a piezo-electric transducer which was driven by a saw tooth wave form. Each time the ball bearing touched the plate a change was observed on the oscilloscope display. In this way a mean value of d could be obtained from several observations. If the width of line was large, the FSR had to be large, necessitating a very small 'd'. If the separation between the plates is less than a few mm, the ball bearing device could not be used. To overcome this difficulty a mercury emission spectrum was used. If the separation between two lines of the Hg spectrum was known, the FSR could be easily calculated. To eliminate the possibility of error in indentifying the lines, the wavelengths of the lines were checked with the help of a Raman spectrometer (Spex Spectrometer).

The instrumental line width (FWHM) is given by

$$\Delta\nu = \frac{FSR}{F} \qquad (2.4)$$

where the parameter F is known as the finesse. The equation (2.4) shows that the minimum frequency spacing of two spectral lines, which can be resolved by FP interferometer is inversely proportional to F. Hence, for maximum resolving power and minimum instrumental width, the finesse should be maximum. A finesse of better than 50 was always attained. The finesse F depends upon several factors; such as, flatness, reflectivity and parallelism of the FP plates.

2.4 The Detection System

The light transmitted by the FP was focussed with a lens on to a pinhole placed in front of the photomultiplier tube (PMT). The PMT used during the work had high sensitivity and a low dark count (~ 1 per second), when cooled thermoelectrically to ~ -20^0C. The output of the PMT was fed to the DAS by way of an amplifier-discriminator.

The DAS-1 was designed, primarily, to record weak spectra for use with a piezo-electrically scanned FP interferometer. It consists of a multichannel analyser of 1024 channels to accumulate the data. The data stored by the multichannel analyser are also used to maintain proper average plate separation and alignment of FP plates. It generates the ramp voltage, which scans the interferometer plate separation through a range of ~ 1000 nm. The same ramp voltage also sequentially addresses the 1024 channels. The optical frequency passed by the interferometer varies linearly with the ramp voltage and thus with channel number. The linear relation between frequency and channel number is independent of the ramp waveform. Data acquisition is prohibited, by logic circuitry, during the fly back portion of the ramp waveform. In the ordinary mode of operation equal time is spent on each channel. The time per channel can be adjusted from 0.01 ms to 99 ms. The DAS-1 also incorporates a provision, known as the segmented time base. It allows the ramp to slow down for a specified region of the spectrum. This helps very much in recording the very weak spectra of CH_4 and CF_4. The Rayleigh line, which was used as a reference line, is an intense line. To record this line, it was swept very fast, but to record the two orders of Raman line the sweeping time in the region of Raman line was 50 to 70 times slower.

Since the ramp addresses both the FP and channel numbers, the display remains linear in frequency.

The other special feature of the DAS is the drift stabilization. It works by locking a narrow and intense Rayleigh line (or other sharp spectral feature) to a given position in the memory. After each sweep the instrument performs a comparison of the number of counts in each half of a programmed window and any tendency of the chosen line to drift from the centre of the window is compensated for by the application of a correction bias to the piezo-electric elements of the interferometer. Finesse optimization was done by a somewhat similar routine as that used for drift stabilization. The procedure for finesse optimization has been thoroughly described by Gammon (1978).

The spectrum can be seen on the CRT display of the DAS. A cursor of the CRT screen can be positioned to address any channel of the memory and the number of counts in that channel are displayed on the screen. When cursor is positioned at channel zero, the total number of sweeps made for recording that particular spectrum is displayed on the CRT screen. The spectrum recorded by the DAS can be recorded on a strip chart recorder.

2.5 Technique

The apparatus described above was used to record the spectra of the Q branch of the ν_1 vibrations of saturated liquid methane (CH_4) and saturated liquid carbon tetrafluoride (CF_4) at temperatures from the triple points to the critical points. The typical gas samples were obtained from Matheson

Gas Products with purity of 99.99% for CH_4 and 99.7% for CF_4. The vapour pressure measurements were made by using a series of three Bourdon tube gauges (accuracies ~ 0.2% and 0.5%) in the range of 1 to 50 bars. These vapour pressure readings were used to adjust the liquid level 2 to 4 mm above the top of the window apertures. All the temperatures were measured employing a platinum resistance theromometer and the values quoted for temperatures at the scattering site are accurate to well within 0.05 K. The calibration of the platinum resistance thermometer was checked by measuring the boiling point of methane. It was further verified that, with the liquid level in sight, all temperatures agreed, within the accuracy of the Bourdon gauges, with those determined from vapour pressure data of CH_4 (NBS Tech. Note 653, (1974)). However, it was difficult to control the liquid level within 1 or 2 K of the critical point. Great care was taken to ensure that the liquid level was always in sight. When the spectrum was being taken the high pressure part of the system was isolated by closing the valve on the top of cryostat. This minimized the gas volume and hence helped to avoid losing liquid each time the temperature was raised. The temperature of the cell was automatically controlled in conjunction with a GaAs sensor. The stability of the temperature control was monitored continuously by recording the output from a differential voltmeter. It was found that the temperature was stable within ~ 0.05 K during the course of an experiment.

The incident radiation beam power was varied from 50 mW to 200 mW, polarized in the direction perpendicular to the scattering plane. Since the spectrum of CF_4 was very weak, the laser power employed was about 200 mW. It took from 15 to 24 hrs. to record a spectrum. The spectrum of CH_4 is quite intense in comparison to that of CF_4. Normally a 3 to 6 hr. spectrum

was found to be satisfactory. The scattered light was collected at an angle of 90^0 to the incident beam. A grating monchromator was used to isolate the vibrational Raman lines.

The scattered light was analysed by the FP interferometer, then collected by the photomultiplier tube. The signal from the photo tube was amplified and pulse shaped and fed to the scaler of the DAS-1. The Raman scattered light was very weak, hence it could not be used by the DAS for drift stabilization or finesse optimization. Therefore the laser line was used as a reference line. A beam splitter was employed to pass a fraction of the beam directly to the interferometer. This beam was passed only for a fraction of the single sweep time. A shutter mechanism, triggered by the DAS was used to control the time interval. All the spectra were recorded by keeping this laser line centered on the drift stabilization and finesse optimization windows. A finesse of better than 50 was always maintained. A mean of two orders of Raman lines was taken to measure the shift and width of the vibrational lines. The 'segmented time base' was always used. This helped in reducing the time to record a spectrum by a factor of at least two or three. Since the width of the ν_1 symmetric vibration of CH_4 was quite large (~ 60 to 120 GHz), a large free spectral range of 574.1 GHz was used, while in case of CF_4 a FSR of 23.812 GHz was used. The FSR had to be chosen so that it avoids excessive inter-order overlap of the wings of the line as well as to minimize instrumental corrections, which became important when the spectral line width approached the instrumental line width. (The instrumental line width was never greater than 10 to 15% of the Raman line).

The spectra of CH_4 and CF_4 were recorded from the triple point to the

critical point. It was attempted to get as close as possible to the triple points and critical points. The full width at half maximum (FWHM) was measured directly on the CRT screen of DAS. The cursor was placed on the peak of each line; the counts on each Raman line were added to the background counts. Half of the sum of the counts was located on each side of the Raman lines and the difference in channel numbers gave the FWHM in channel numbers. An average of two orders was taken and then the width was converted into GHz. A detailed procedure for measuring width and shift of the Raman lines has been described by Ali (1978). The shift was measured from the triple point density to the critical point density, assuming the frequency shift to be zero at the triple point density. Care was taken that for a change in temperature the order of the Raman spectrum was always the same.

CHAPTER - III

EXPERIMENTAL RESULTS AND DISCUSSION

The polarized, or isotropic contributions to the totally symmetric (ν_1) vibrational Raman spectra of methane and carbon tetrafluoride were measured in the liquid phase along the liquid-vapour coexistence line from the triple point to the critical point in each case. (Values of the relevant physical constants and fundamental vibrational frequencies of CH_4 and CF_4 are given in table 3.1). Attention was focussed on three principal characteristics of the single component spectra: (1) the line width, i.e. full width at half maximum, Γ, (2) the shift in peak frequency relative to that at the triple point, $\nu - \nu_\rho$, in the spectra and (3) the degree of asymmetry observed in the line shape. Typical spectra of CH_4 are shown in Fig. 3.1. These spectra were recorded at near triple point, boiling point and critical point. The line width at the triple point and boiling point is almost the same (~ 73 GHz), while at the critical point it increases by a factor of ~ two (117.2 GHz). The line is asymmetric near the triple point and critical point, but the asymmetry is in opposite direction at the triple point to that at the critical point. The line is symmetrical at the boiling point. The intensities of the lines are in arbitrary units.

3.0 Line Widths

The vibrational Raman line widths (FWHM) as measured throughout the saturated liquid ranges of CH_4 and CF_4 are given in Table 3.2. These widths were plotted against the temperature T. The variation of line widths with temperature is depicted graphically in Figs. 3.2 and 3.3.

TABLE 3.1

A. Physical Constants of CH_4 and CF_4

	CH_4	CF_4
Molecular Weight,	16.043 gm/mole	88.01 gm/mole
Triple Point Temperature	90.68 K	89.16 K
Boiling Temperature	109 K	145.16 K
Critical Temperature	190.55 K	227.7 K
Critical Pressure	46.6 atm	36.9/atm
Critical Density	223.46 Amagat	164.1 Amagat

B. Fundamental Vibrational Frequencies of CH_4 and CF_4

	CH_4	CF_4
	cm^{-1}	cm^{-1}
ν_1	2916.7 (R)	904 (R)[a]
ν_2	1533.6 (R)	437 (R)
ν_3	3018.9 (R,IR)	1283 (R,IR)[b]
ν_4	1306.2 (R,IR)	630 (R,IR)

a. R-Raman allowed

b. IR-Infrared allowed

Figure 3.1

Typical experimental polarized spectra for the ν_1 symmetric vibrational Raman line of CH_4 at three different temperatures

i) Near Triple Point 90.72 K

ii) Near Boiling Point 111.7 K

iii) Near Critical point 190.50 K

The intensities of the spectra are in arbitrary units.

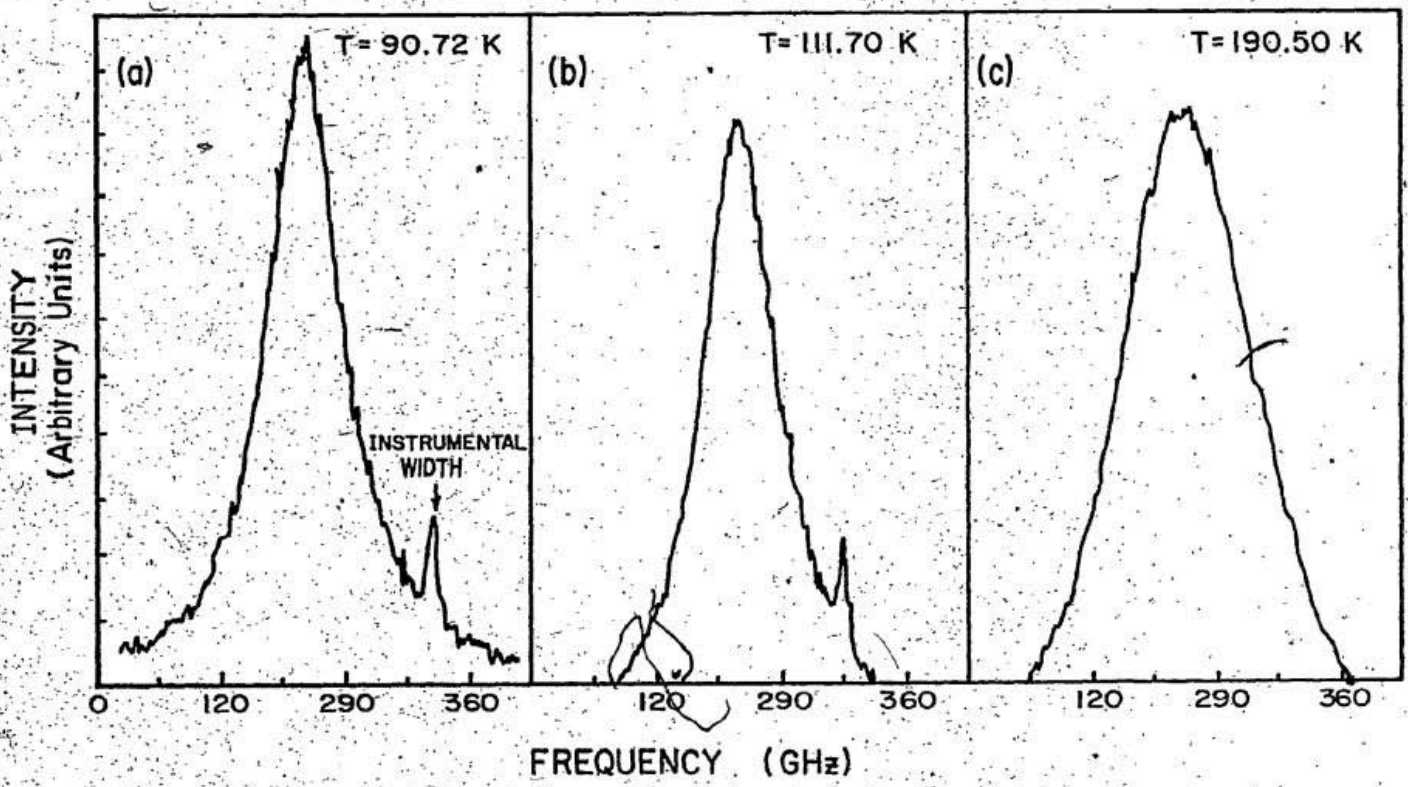
(a)
T= 90.72 K
(b)
T= 111.70 K
(c)
T= 190.50 K
INSTRUMENTAL WIDTH
INTENSITY (Arbitrary Units)
0
120
290
360
120
290
360
120
290
360
FREQUENCY (GHz)

Fig. 3.I

TABLE 3.2

Data for Raman Vibrational linewidth (FWHM), Γ, for saturated liquid CH_4 and CF_4 from their triple points to critical points.

Methane		Carbon Tetrafluoride	
Temperature (K)	Γ (GHz)	Temperature (K)	Γ (GHz)
90.72	72.8	89.18	7.9
93.05	71.6	90.35	7.5
99.08	72.4	92.20	7.3
104.91	75.0	95.67	6.9
105.40	75.0	98.03	6.6
111.70	73.6	104.59	6.2
115.07	75.4	115.55	5.2
123.07	74.2	126.88	5.0
128.28	73.2	137.41	4.5
135.17	75.8	147.94	4.3
140.23	74.4	158.63	4.2
144.29	75.6	164.95	4.3
149.30	72.4	170.31	4.3
154.28	75.8	180.10	4.0
159.40	76.0	187.05	4.1
164.40	77.0	194.65	4.3
168.50	79.6	201.21	4.2
172.61	82.1	207.55	4.1
177.21	84.0	214.37	4.3
182.02	84.4	218.09	4.0
183.85	87.6	219.93	3.9
186.16	92.3	221.87	3.9
187.16	91.7	224.01	4.0
188.47	98.9	226.21	4.0
189.36	98.7	226.52	4.3
189.52	102.0	227.17	4.0
189.87	104.5	227.40	4.0
190.06	107.5		
190.10	111.8		
190.26	115.8		
190.46	115.4		
190.50	117.2		

Figure 3.2

Plot of full width at half maximum (FWHM), Γ, of the Raman Q branch vs temperature from the triple point to the critical point for the saturated liquid methane.

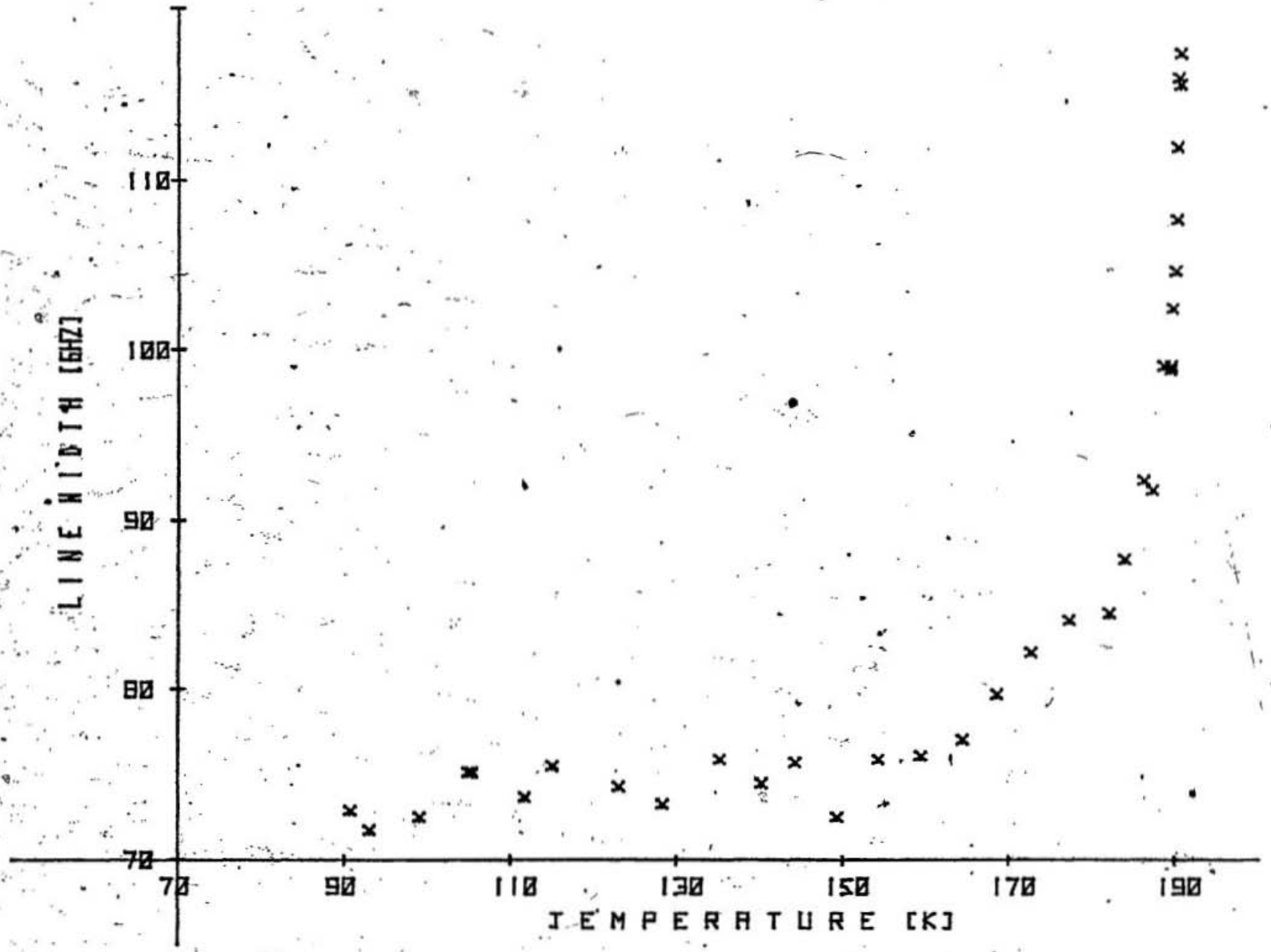
LINE WIDTH [GHZ]
110
100
90
80
70
70
90
110
130
150
170
190
TEMPERATURE [K]

Fig. 3.2

Figure 3.3

Plot of full width at half maximum (FWHM), Γ, of the Raman Q branch vs temperature from triple point to critical point for saturated liquid carbon tetrafluoride (CF_4).

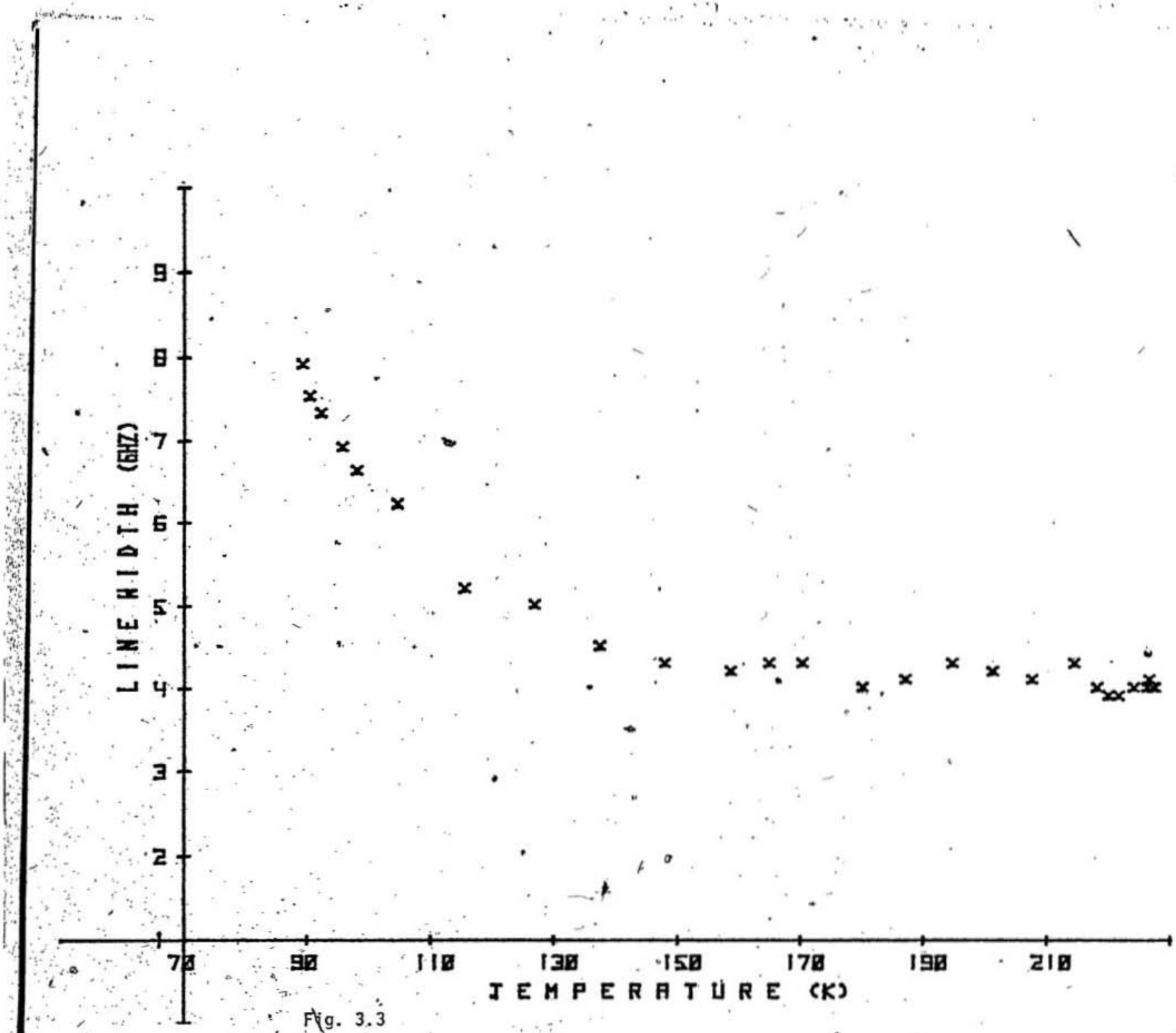
LINE WIDTH (GHZ)
2
3
4
5
6
7
8
9
70
90
110
130
150
170
190
210
TEMPERATURE (K)

Fig. 3.3

In Fig. 3.4, linewidths of N_2, O_2 (Clouter and Kiefte, 1977), CO (Clouter et al.). CH_4 and CF_4 are plotted against temperature T. From Fig. 3.4 it can be seen that the line width increases from the boiling point to the triple point in case of O_2, CF_4, CO and N_2. The incremental change in linewidths is more pronounced in case of O_2, CF_4 and CO, while, there is no variation in line width of CH_4 near the triple point to the boiling point. The line widths of N_2, O_2, CO and CH_4 increase above the boiling point and reach a maximum value at near critical point. It is interesting to note that in case of CF_4 the linewidths remain constant from the boiling point to the critical point.

As mentioned in Chapter I, Brueck (1977) has shown that motional narrowing contributes significantly to the polarized vibrational Raman lines of N_2, O_2 and CO. But for the reasons described in Chapter I, motional narrowing does not contribute to the linewidths in the case of CH_4. Hence this effect will not be considered here and it is assumed that the line width is mainly due to vibrational relaxation. Phase relaxation and energy relaxation are the two most important processes in vibrational relaxation. In the case of CH_4, phase relaxation is believed to play the main role in the line broadening mechanism, since the energy gap between the ground state and the lowest excited vibrational state is comparable to that for N_2. It is reminded that in case of N_2, the ratio of vibrational life time to the dephasing time is 10^{10} (Laubereau, 1974). This ratio varies from molecule to molecule; in case of C_2H_5OH it is 80, whereas a value of 4 was estimated for CH_3CCl_3 by Laubereau et al., (1972). Fischer and Laubereau (1975) have considered energy dissipation and pure dephasing to be approximately independent processes, and assumed that the dephasing time τ can be

Figure 3.4

Plots of full width at half maximum (FWHM), Γ, of the Raman Q branch vs temperature from the triple point to the critical point of the saturated liquids, N_2, O_2, CO, CF_4 and CH_4.

The triple points and critical points for N_2, O_2, CO, CF_4 and CH_4 are as follows:

Sample	Triple Point (K)	Critical Point (K)
N_2	63.3	126.25
O_2	54.76	154.57
CO	74.16	132.85
CF_4	89.16	227.7
CH_4	90.68	190.56

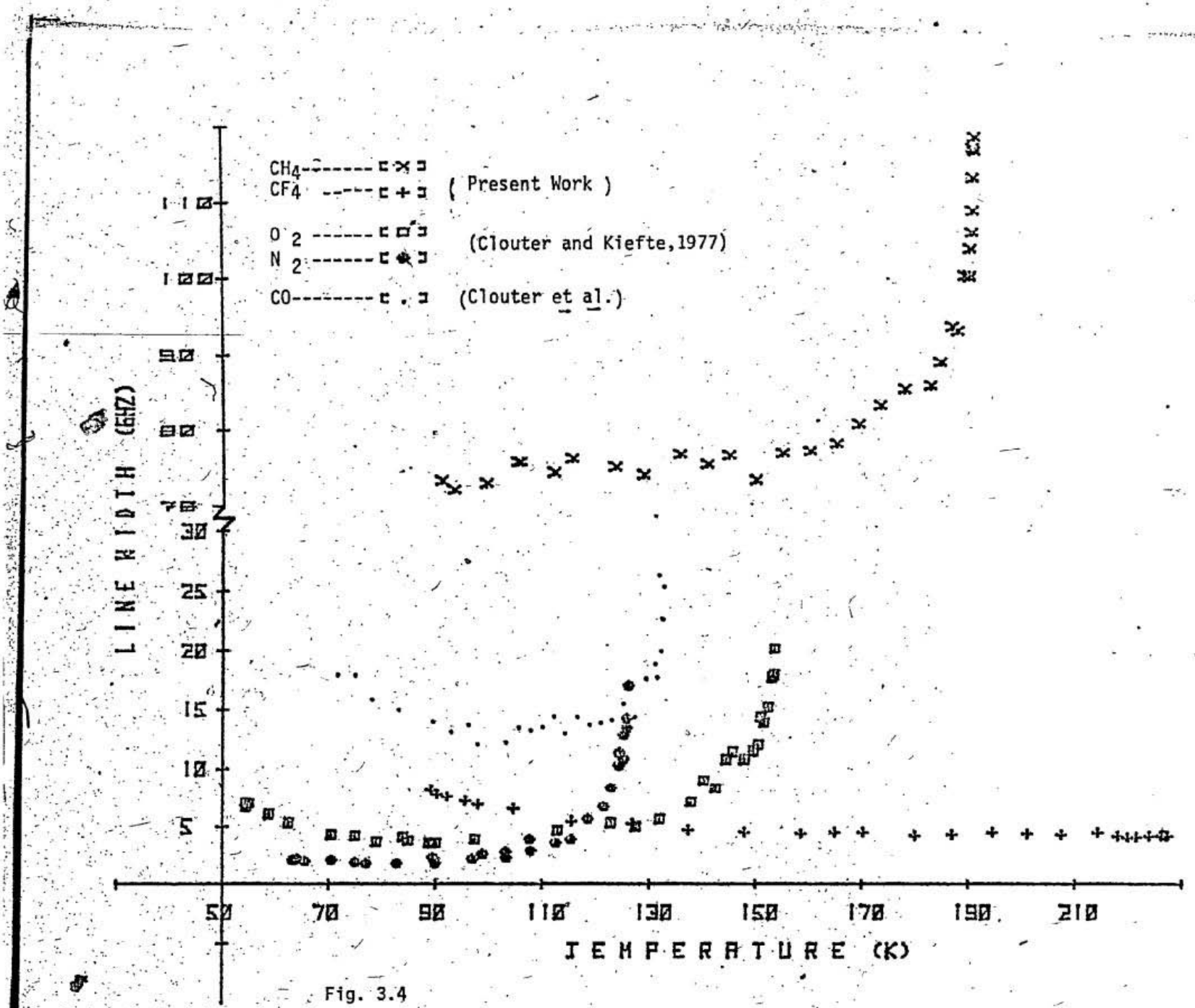
CH4 ------
CF4 ------ (Present Work)
O 2 ------
N 2 ------ (Clouter and Kiefte,1977)
CO -------- (Clouter et al.)
LINE WIDTH (GHZ)
TEMPERATURE (K)
50
70
90
110
130
150
170
190
210
5
10
15
20
25
30
100
110

Fig. 3.4

represented as

$$\frac{1}{\tau} = \frac{1}{\tau_2} + \frac{1}{\tau_1} \qquad (3.1)$$

where τ_1 is the energy relaxation time and τ_2 corresponds to pure dephasing by which the excited state population of the vibrational mode is not affected. In many of the liquids, such as N_2, O_2, CH_3CCl_3, CH_3CH_2OH (Laubereau, 1975), $CHCl_3$ and $CDCl_3$ (Schroeder et al., 1977), experimental data indicate that $\tau_2 \simeq \tau$. Therefore it is also assumed that the line width is mainly due to phase relaxation in CH_4 and CF_4.

The line width measurements are divided into two parts: i) from the triple point to the boiling point and ii) from the boiling point to the critical point. In this section, the measurements of line width from the triple point to the boiling point will be considered. The region from the boiling point to the critical point for each liquid CH_4 and CF_4 will be dealt with separately in later sections. In the case of CH_4, there is no significant variation in line width from the triple point to the boiling point, while in case of CF_4 the line width decreases by a factor of $\simeq 2$ from the triple point to the boiling point. In this region CF_4 behaves similar to that of O_2. No detailed theory is available in the literature, which deals with line widths at and above the triple point. It might be remarked that orientational ordering could contribute to the line width. Crawford, Daniels and Ching (1975) have discussed molecular orientations in liquid CH_4. They have suggested that there may be a greater local orientational order in liquid than in solid CH_4 near the melting point. The reason could be attributed to the lowering of the fluid's internal energy relative to the solid.

3.1 Asymmetry

Figs. 3.5 and 3.6 show the variation in degree of asymmetry of Raman line shapes with temperature. Prior to this work, no one has attempted to determine the asymmetry in Raman vibrational line shapes. Because of experimental problems, no attempt was made to obtain a computer fit of the line shapes. Hence the degree of asymmetry was determined only qualitatively. The asymmetry was calculated as the ratio of halfwidth at half maximum on the lower wavelength side to half width at half maximum on the higher wavelength side. Hence for a symmetrical line shape the ratio should be one. In both the liquids, CH_4 and CF_4, near the triple point the line width is asymmetric and in opposite direction to the asymmetry near the critical point. In the case of CH_4 the line shape is symmetrical from above the triple point to about 20 K below the critical point. In this region, there is no variation in linewidth. Within 20 K of the critical point the linewidth begins to increase at the same time asymmetry also starts to increase. Similarly for CF_4, we observe that the line shape is symmetrical from somewhat above the triple point to within a few degrees K from the critical point. The asymmetry is maximum at the critical point. From the above observations it is obvious that asymmetry has to be taken into account to calculate the line shape or width. So far no author has tried explicitly to consider the effects which cause the line to be asymmetric. On the experimental side it would be more fruitful to determine the exact line shapes for the entire range of temperature from the triple point to the critical point.

Figure 3.5

Plot of asymmetry of ν_1 symmetric Raman vibrational line vs. temperature for saturated liquid CH_4.

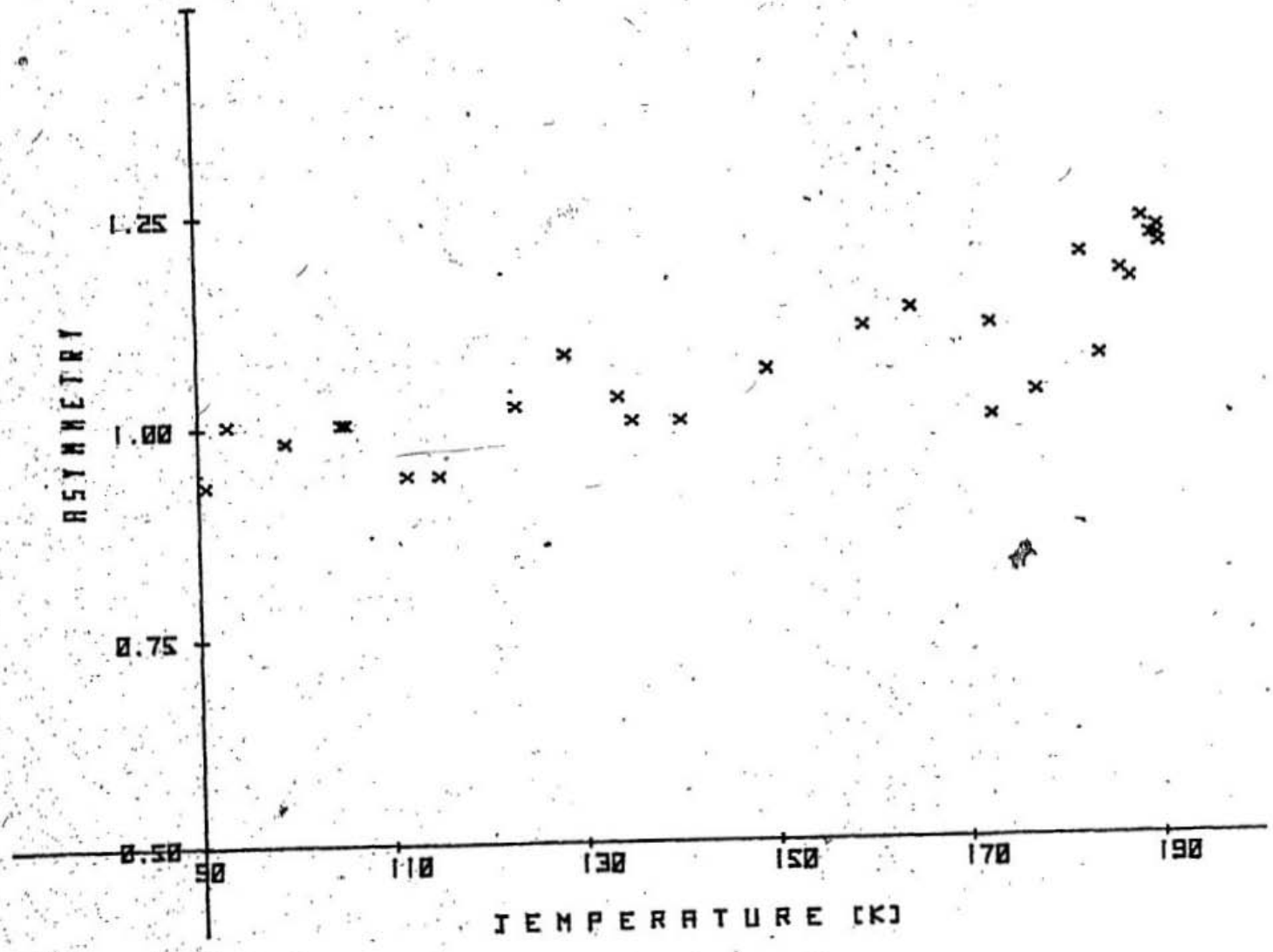
1.25
1.00
0.75
0.50
ASYMMETRY
90
110
130
150
170
190
TEMPERATURE [K]

Fig. 3.5

Figure 3.6

Plot of asymmetry of ν_1 symmetric Raman vibrational line vs. temperature for the saturated liquid CF_4.

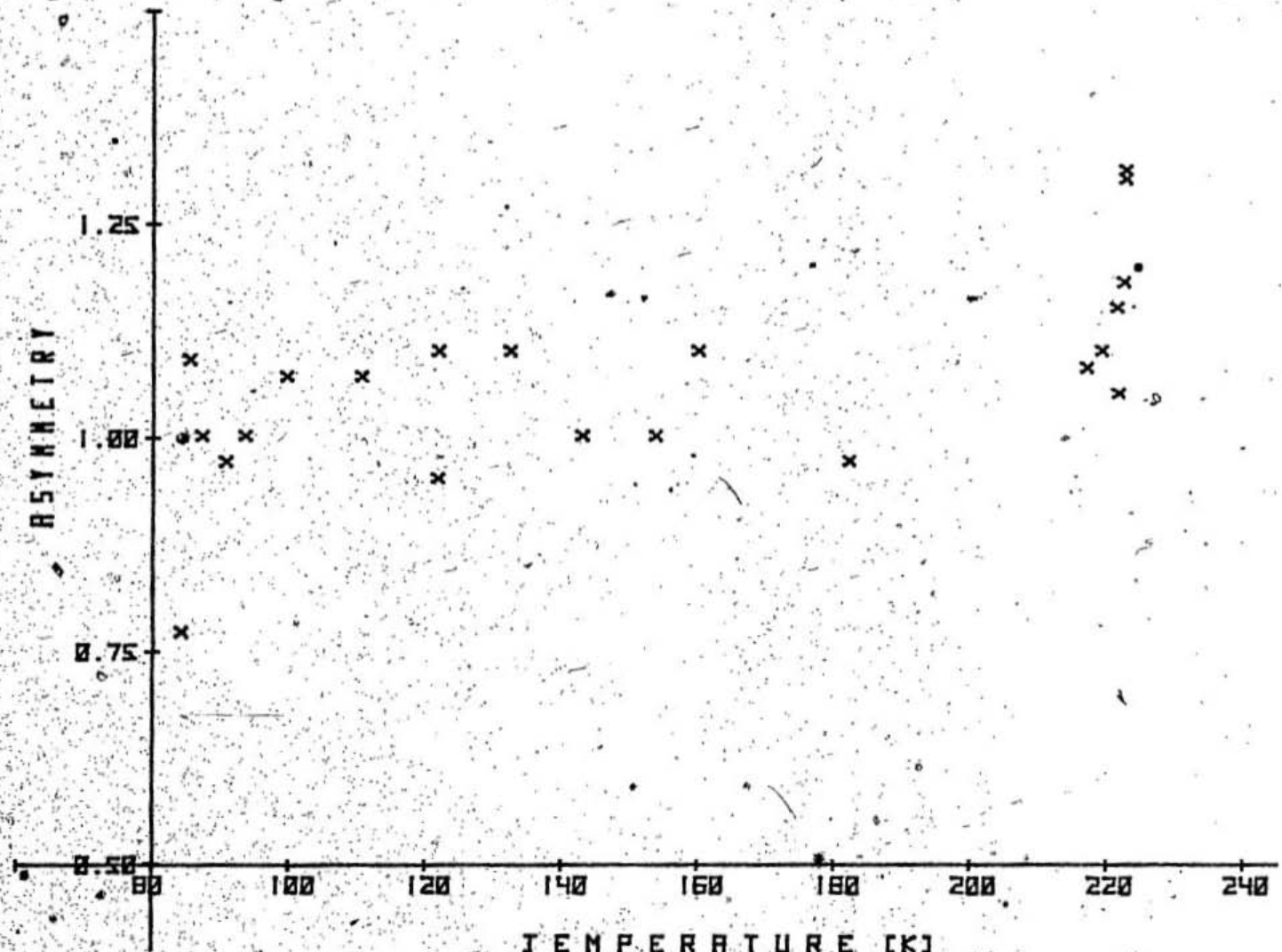
1.25
1.00
0.75
0.50
ASYMMETRY
80
100
120
140
160
180
200
220
240
TEMPERATURE [K]

Fig. 3.6

3.2 Frequency Shift

From the Figs. 3.7 and 3.8, it is seen that the relative Raman frequency shift varies linearly with density in both the liquids CH_4 and CF_4. The data for relative shifts are presented in Tables 3.4, 3.5 for CH_4 and CF_4. To calculate the relative frequency shift the peak position of the Raman lines at the triple point was taken to be zero and all the peak frequencies from triple point onwards were subtracted from it. Liquid density data were determined using the published PVT data for CH_4 by Goodwin (1974) and for CF_4 from tables by Landolt-Bornstein. In case of CF_4 the relative Raman frequency shift varies linearly approximately. Because of the extremely weak spectrum of CF_4, there is little more uncertainty in peak frequency measurement of CF_4 vibrational lines than that of CH_4. The data for density of CF_4 are also not very accurate.

In the gas phase, the shift of the vibrational Raman lines arises from the perturbations of molecules by the isotropic intermolecular forces. Bhatnagar et al. (1962) and May et al. (1964) studied experimentally the frequency shift of the individual Q-branch components of compressed H_2 molecules. Gray and Van Kranendonk (1966) considered this problem theoretically and showed that anisotropic forces do not contribute to the shift of the lines. The Raman shifts can be expressed in a 'virial type' expansion in powers of the density:

$$[Q(J)]_\rho = Q(J) + a_J \rho + b_J \rho^2 \qquad (3.2)$$

where $Q(J)$ is the Raman frequency of the free molecule and a_J and b_J are

Figure 3.7

Plot of relative Raman frequency shift ($\nu - \nu_{tp}$) vs. density (ρ) for the saturated liquid CH_4.

FREQUENCY SHIFT (GHZ)
0
02
04
06
08
01
12
14
16
18
DENSITY (AMAGAT)
225
275
325
375
425
475
525
575
625

Fig. 3.7

Figure 3.8

Plot of relative Raman frequency shift ($\nu - \nu_{tp}$) vs. density (ρ) for saturated liquid CF_4.

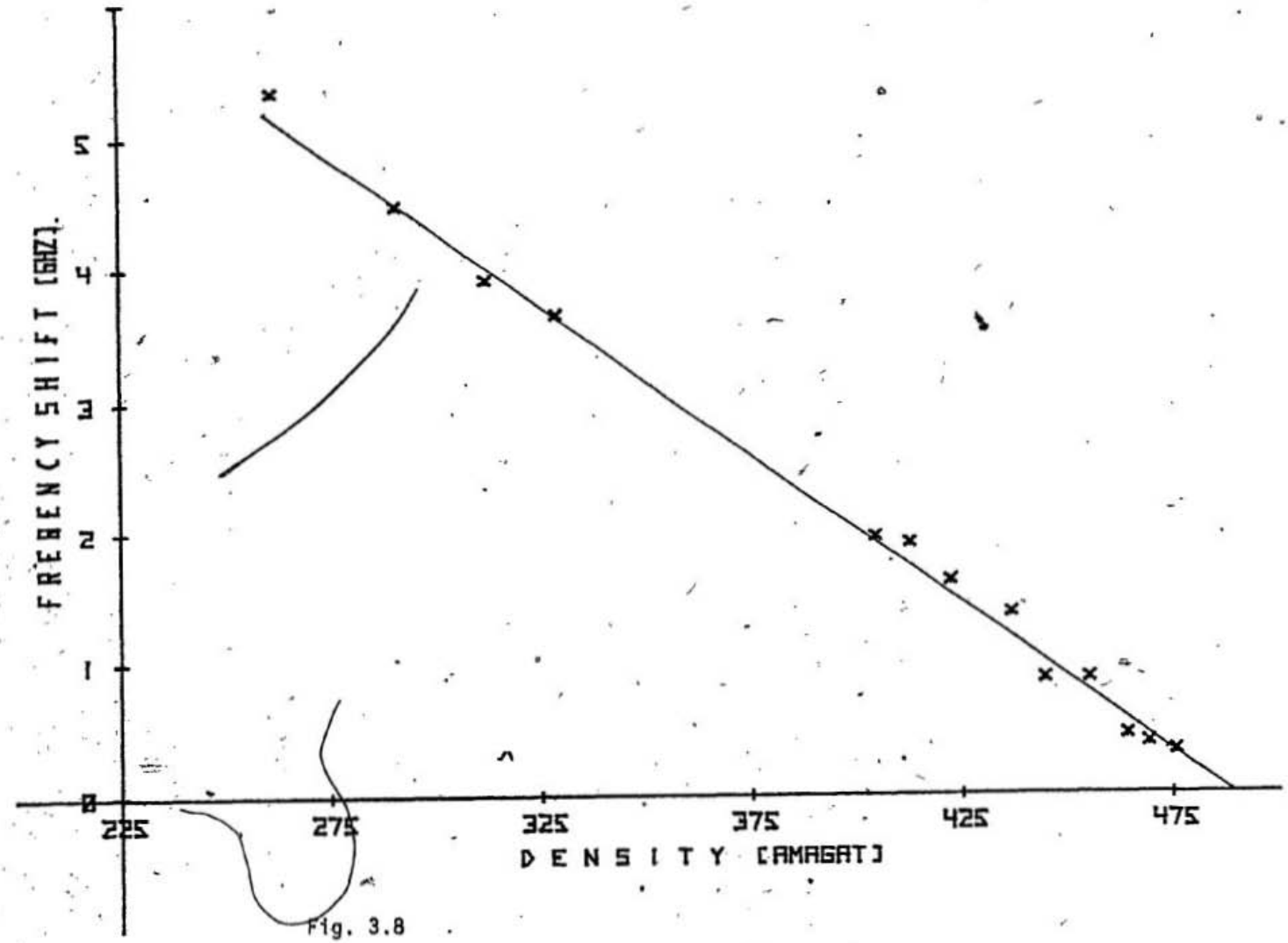
FREQUENCY SHIFT [GHZ].
0
1
2
3
4
5
225
275
325
375
425
475
DENSITY [AMAGAT]

Fig. 3.8

TABLE 3.4

List of relative Raman frequency shift ($\nu - \nu_{tp}$) and density (ρ) at temperatures from the triple point to the critical point for saturated liquid CH_4.

Temperature (K)	Density ρ(Amagat)	Relative Frequency shift ($\nu - \nu_{tp}$) (GHz)
90.72	629.61	0.00
93.05	625.29	4.44
99.08	613.92	9.65
104.91	602.69	13.67
111.70	589.19	20.90
123.07	565.34	33.77
128.28	553.79	38.09
133.71	541.22	46.03
139.13	528.04	53.33
144.29	514.89	61.41
149.30	501.36	67.86
154.28	487.08	79.76
159.36	471.41	88.06
164.40	454.46	96.14
168.50	439.29	106.55
172.61	423.75	112.30
177.21	400.58	122.01
182.02	372.61	131.70
183.85	359.51	140.60
186.16	339.72	149.83
189.41	294.97	172.26
189.52	293.03	175.39
189.87	286.87	181.02
190.03	281.30	184.26
190.10	273.62	186.25
190.26	256.07	188.94
190.36	245.10	196.28
190.46	234.13	197.60
190.50	229.75	198.93

TABLE 3.5

List of relative Raman frequency shift ($\nu - \nu_{tp}$) and density (ρ) at temperature from the triple point to the critical point for saturated liquid CF_4.

Temperature (K)	Density ρ(Amagat)	Relative Frequency shift ($\nu - \nu_{tp}$) (GHz)
89.18	477	0.0
90.35	475	0.31
98.03	469	0.37
104.59	464	0.43
115.55	455	0.85
126.88	444	0.85
137.41	436	1.35
147.94	422	1.60
158.63	412	1.89
164.95	404	1.94
194.65	340	3.47
201.21	328	3.63
207.55	312	3.89
214.37	290	4.46
218.09	261	5.33

J-dependent and temperature dependent constants and J is given rotational state.

Only a couple of experiments have been done to measure the frequency shift in different liquids (Clouter et al.)* along the liquid-vapour co-existence line. In all the liquids N_2, O_2, CO, CH_4 and CF_4 the Raman shifts vary linearly with density. In the gas phase the theory is simple and straightforward, but for liquids the strong correlation effects should also be incorporated.

3.1 The Vibrational Raman Spectra of Liquid Methane from Boiling Point to Critical Point

The vibrational dephasing has been theoretically studied in detail by Hills and Madden (1978, 79). They have described a model to explain the experimental results obtained by Clouter and Kiefte (1977) for temperature dependence of N_2 and O_2 from the boiling point to the critical point. To explain the results obtained for CH_4 and CF_4 the theory developed by these authors for N_2 and O_2 will be used in this thesis.

When a beam of monochromatic light is passed through a dense transparent fluid some of the light is scattered. Since the density is not uniform, the density fluctuations in a fluid are time dependent. This means that the frequency of light scattered by density fluctuations in a dense fluid exhibits a spectrum characteristic of the time dependence of the density fluctuations. The density fluctuations can be described by the dynamic structure factor $S(Q, \omega)$. A molecule relaxes by interacting with the density fluctuations in the fluid surrounding it. Hills and Madden (1978)

have shown that the local dynamic structure factor of the fluid governs the rate of vibrational dephasing. Further, they have pointed out that the first peak in the structure factor S(Q) contributes significantly to vibrational dephasing, well away from the critical point, while the density fluctuations with small wave vector and frequency do not make any appreciable contribution to the vibrational relaxation. However, near the critical point the isothermal compressibility becomes very large (infinite at critical point) and it allows the density fluctuations to grow to large amplitude (Fisher, 1964). This causes increases in the rate of vibrational relaxation rate. Hence there is an increase in line width.

Hills and Madden (1979) showed that the vibrational Raman full width at half height Γ can be expressed as:

$$\Gamma = 2\rho_e \lim_{\omega \to o} \sum_L B_L \int_0^\infty dQ\, Q^2\, S(Q, \omega)\, V_L^2(Q) \qquad (3.3)$$

and

$$V_L(Q) = \int_b^\infty dr\, r^2\, j_L(Qr)\, R_L(r) \qquad (3.3a)$$

where ρ_e is the equilibrium fluid density, B_L contains molecular constants, L is the rank, which decides how the probe-molecule-fluid interaction transforms under rotation. e.g. isotropic dispersion forces would correspond to an L value of zero, "b" is effective radius of molecule and $j_L(Qr)$ is the modified Bessel function. The intermolecular potential $V_L(Q)$ determines which Q Fourier components of the density fluctuations are most effective in causing the relaxation. The dynamical structure factor $S(Q, \omega)$ (Stanley, 1971) is given, in the simplest approximation, by:

$$S(Q, \omega) = \frac{K_T}{\pi (K_T)_o} \left(\frac{\kappa^3}{\kappa^2 + Q^2}\right) \left(\frac{\Gamma_A}{\omega^2 + \Gamma_A^2}\right) \tag{3.4}$$

where $\Gamma_A = D_T Q^2$ (3.5)

κ is the inverse correlation length (Orenstein-Zernicke)

and $D_T = \frac{\lambda}{\rho_e C_p}$, where λ is thermal conductivity and D_T (3.6)

is the thermal diffusivity. Hills and Madden (1979) obtained the following expression for the critical contribution to the line width

$$\Gamma = A \frac{K_T}{(K_T)_o} \kappa^3 \lim_{\omega \to o} \left\{\left(\frac{\phi}{\omega^2 + \phi^2}\right) + \left(\frac{|\omega|}{2\phi}\right)^{1/2} \times \left(\frac{\omega - \phi}{\omega^2 + Q^2}\right)\right\} \tag{3.7}$$

where $\phi = \kappa^2 D_T$ (3.8)

In the fast motion limit ($\omega \to o$) and $\omega \phi^{-1} \ll 1$

They obtained

$$\Gamma = A \frac{K_T}{(K_T)_o} \frac{\kappa}{D_T} . \tag{3.9}$$

Substituting (Stanley, 1971) $\frac{K_T}{(K_T)_o} = \frac{4}{9} \varepsilon^{-\gamma}$, $\kappa = \kappa_o \varepsilon^{\nu}$ and $D_T = D_o \varepsilon^{\gamma - a}$, where $\varepsilon = \frac{|T - T_c|}{T_c}$ and γ, ν and 'a' are critical exponents. One obtains the exponent for eq. (3.9) to be $(-2\gamma + \nu + a)$. However, this condition is not applicable in case of CH_4 since $\omega \phi^{-1}$ is greater than one (see table 3.6). In the limit $\ell n\, \varepsilon < -2.5$, $\omega \phi^{-1} \gg 1$ and making ω ($\omega \sim \Gamma$) a small positive constant $\bar{\varepsilon}$, (>0) the equation (3.9) has exponent equal to $(-\frac{3}{2}\gamma + 2\nu + \frac{a}{2})$.

The above relation was obtained assuming the line shape to be Lorentzian. The conditions for relaxation phenomena and line shape problems have been discussed by Kubo (1961). A brief account of the line shape problem has already been given in Chapter I.

At this point, a few lines about critical exponents would not be out of place. The hypothesis of universality of critical phenomena states that for systems exhibiting critical point, phase transitions can be grouped into universality classes. These systems are expected to have the same critical exponents. These exponents have been calculated theoretically by many techniques. The various calculations yield numerically similar results. For few substances, these have also been determined experimentally. The most recent measurements have been made by Chang et al. (1979) for a binary liquid mixture (3-methylpentane-nitroethane). They have reported the following values:

$$\gamma = 1.235 \pm .016$$

and

$$\nu = 0.625 \pm .006$$

The value for the critical exponent 'a', for CO_2, has been determined only by Swinney and Cummins (1968). They have found the value of 'a' to be 0.53. However, for methane the value for the critical exponent γ has been obtained by Jansoone et al. (1970). They have reported it to be 1.287. Hence to calculate the numerical value of the exponent $(-\frac{3}{2}\gamma + 2\nu + \frac{a}{2})$, the following values of γ, ν and a were used

$$\gamma = 1.287$$
$$\nu = 0.625$$
$$a = 0.53$$

This comes out to be -0.41 for methane. Hills and Madden (1979) used the values $\gamma = 1.25$, $\nu = \frac{2}{3}$ and $a = 0.52$; this gives $(-\frac{3}{2}\gamma + 2\nu + \frac{a}{2}) = -0.28$. These authors, therefore, argued that the theoretical value of -0.28 agreed very well with the experimental value of -0.3 for N_2 and O_2. In their deduction for Γ they did not, however, include the contribution of motional narrowing (Brueck, 1977). Even without considering the effect of motional narrwoing and using the simple classical expression for $S(Q, \omega)$, they were able to show good agreement between theory and experiment. The agreement obtained may therefore be a fortuitous consequence of having applied a simple classical approximation for $S(Q, \omega)$ while neglecting the effect of motional narrowing. This point of view is further supported by the arguments which follow.

In the Table 3.6, numerical values for $\omega\,\phi^{-1}$ have been given. It is seen that for methane $\omega\,\phi^{-1}$ is always greater than one, while in case of N_2 and O_2, $\omega\,\phi^{-1}$ has both values i.e. <1 and >1 (Hills and Madden 1979). Therefore it is assumed that one would get experimental values for the critical exponent $(-\frac{3\gamma}{2} + 2\nu + \frac{a}{2})$ close to -0.41 for methane. But from the Fig. 3.9 (plot of $\ell n\,\Gamma$ vs $\ell n\,\varepsilon$), it is seen that in case of CH_4 the value of slope is only -0.09. Thus one finds that the expression derived by Hills and Madden (1979) can not be applied for methane.

One needs to consider the dynamical structure factor $S(Q, \omega)$ in more detail (Krynicki et al. 1977). In the equation (3.5) $\Gamma_A = D_T Q^2$, but when $Q >> \kappa$ the basic assumption underlying the hydrodynamic theory (that $Q << \kappa$) is no longer valid. Therefore in the region $Q >> \kappa$, the expression

TABLE 3.6

Estimation of $\omega\phi^{-1}$ for liquid CH_4

Temperature (K)	Half Width ω (GHz)	$(T_c-T)/T_c$ ε	ϕ $\phi(=100\varepsilon^2$ GHz)	$\omega\phi^{-1}$
115.07	75.4	3.96E-01	1.57E 01	4.80E 00
123.07	74.2	3.54E-01	1.25E 01	5.91E 00
128.28	73.2	3.27E-01	1.07E 01	6.85E 00
135.17	75.8	2.91E-01	8.45E 00	8.97E 00
140.23	74.4	2.64E-01	6.97E 00	1.07E 01
144.29	75.6	2.43E-01	5.89E 00	1.28E 01
149.30	72.4	2.16E-01	4.69E 00	1.54E 01
154.28	75.8	1.90E-01	3.62E 00	2.09E 01
159.40	76.0	1.63E-01	2.67E 00	2.84E 01
164.40	77.0	1.37E-01	1.88E 00	4.09E 01
168.50	79.6	1.16E-01	1.34E 00	5.94E 01
172.61	82.1	9.42E-02	8.87E-01	9.26E 01
177.21	84.0	7.00E-02	4.90E-01	1.71E 02
182.02	84.4	4.48E-02	2.01E-01	4.21E 02
183.85	87.6	3.52E-02	1.24E-01	7.08E 02
186.16	92.3	2.31E-02	5.32E-02	1.73E 03
187.16	91.7	1.78E-02	3.17E-02	2.89E 03
188.47	98.9	1.09E-02	1.20E-02	8.26E 03
189.41	98.9	6.01E-03	3.61E-03	2.74E 04
189.36	98.7	6.27E-03	3.93E-03	2.51E 04
189.52	102.3	5.43E-03	2.95E-03	3.47E 04
189.87	104.5	3.59E-03	1.29E-03	8.09E 04
190.06	107.5	2.60E-03	6.75E-04	1.59E 05
190.10	111.8	2.39E-03	5.70E-04	1.96E 05
190.26	115.8	1.55E-03	2.40E-04	4.83E 05
190.46	115.4	4.99E-04	2.49E-05	4.64E 06
190.50	117.2	2.89E-04	8.33E-06	1.41E 07

Figure 3.9

Plot of logarithm (base e) of FWHM($\ell n\Gamma$) of the vibrational Raman spectrum of liquid CH_4 against the logarithm of the reduced temperature, ($\ell n\epsilon$), $\epsilon = [|T - T_c|/T_c]$.

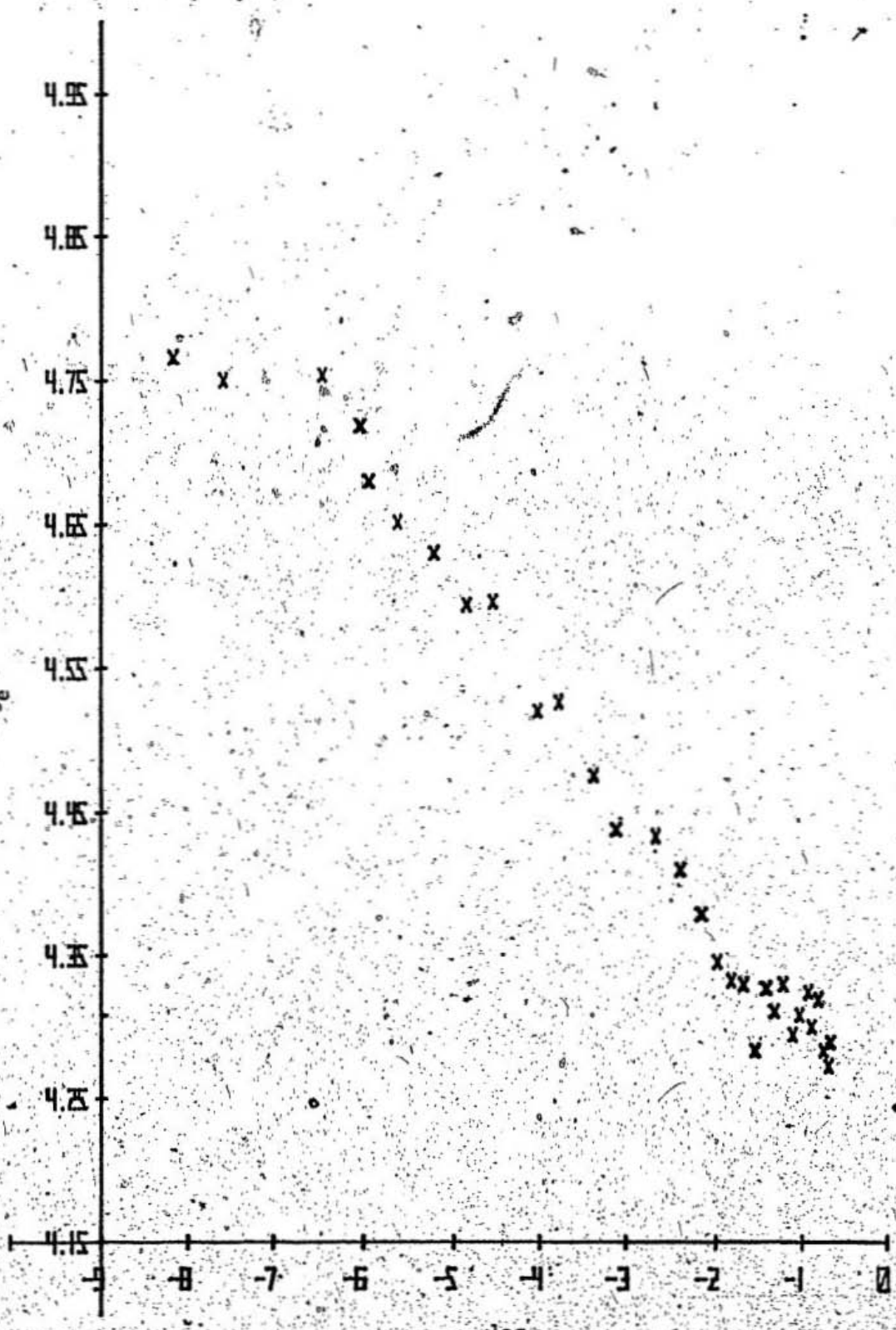

Fig. 3.9

for Γ_A given by Kawasaki (1970) should be used i.e.

for

$$Q > \kappa,\ \Gamma_A = \frac{3}{8}\pi D_T Q^2 \left[\frac{Q}{\kappa} + \frac{8}{3\pi}\left(\frac{\kappa}{Q}\right)^2 + \ldots\right] \tag{3.9}$$

Swinney and Cummins (1968) have also found that near the critical point $\Gamma_A = D_T Q^2$ is no longer valid and they used the expression

$$\Gamma_A = D_T Q^2 \left[1 + B\left(\frac{Q}{\kappa}\right)^2\right] \tag{3.10}$$

to find out the value of critical exponent 'a'.

If we retain the first term in the expression (3.9), then use (3.4) in (3.3), making ω a small positive constant $\bar{\varepsilon}$ and using the condition $\omega\,\phi^{-1} >> 1$, we get (Krynicki et al., 1977)

$$\Gamma \propto \frac{K_T}{(K_T)_0}\ \frac{\kappa}{D_T}\ \left(\frac{\varepsilon}{D_T\kappa^2}\right)^{-\frac{2}{3}} \tag{3.11}$$

Using the relation for $\frac{K_T}{(K_T)_0}$, κ and D_T, it is found that

$$\Gamma \propto \varepsilon^{-\left(\frac{4}{3}\gamma + \frac{7}{3}\nu + \frac{a}{3}\right)} \tag{3.12}$$

On substituting the values for γ, ν and a, one obtains

$$\Gamma \propto \varepsilon^{-0.08} \tag{3.13}$$

The calculated value of -0.08 agrees very well with the experimental slope of (Fig. 3.9) of -0.09. With $T_c - T < 0.2$ K, the slope of curve

($\ell og_e \Gamma$ vs $\ell og_e \varepsilon$) has a value close to zero. At these temperatures, the critical fluctuations would be very slow so that their dynamical behaviour can be neglected. That is, ϕ can be taken to be zero for very small ε (see table 3.6). As pointed out by Hills and Madden (1979) this situation corresponds to the 'rigid-lattice' limit. (This will be discussed in detail in the next section). In this limit $\Delta\tau_c >> 1$ and the slope has a zero value. Hence it is seen that the observed line width for methane can also be explained theoretically.

3.4 The Vibrational Raman Spectra of Liquid Carbon Tetrafluoride from the Boiling Point to the Critical Point.

The ν_1 symmetric vibrational mode of CF_4 is found to be relatively insensitive in the region from the boiling point to the critical point. This may be an indication that the contribution from vibrational dephasing is very small. From Fig. 3.4 it is seen that CF_4 behaves differently from all other liquids CO, N_2, O_2 and CH_4 in the region considered in this section.

It is assumed that the line shape is Lorentzian. It is unfortunate that no one has attempted to calculate or determine experimentally the correlation time τ_c for liquid CF_4. Therefore it can not be said with certainty that the line shape is Lorentzian. But since the linewidth could be explained on the basis of the theory proposed by Hills and Madden (1979), it is not unreasonable to assume the line shape to be Lorentzian. The equation (3.9) was obtained under the condition $\omega << \phi$ and $\omega \to 0$. In case of CF_4 (table 3.7) $\omega \phi^{-1} \sim 1$, in the temperature range form 147 K to 187 K,

TABLE 3.7

Estimation of $\omega \phi^{-1}$ for saturated liquid CF_4

Temperature (K)	Half Width ω (GHz)	$(T_c-T)/T_c$ ε	ϕ $(=100\ \varepsilon^2)$ GHz	$\omega \phi^{-1}$
147.94	4.3	3.50E-01	1.22E 01	3.51E-01
158.63	4.2	3.03E-01	9.16E 00	4.57E-01
164.95	4.3	2.75E-01	7.56E 00	5.67E-01
170.31	4.3	2.51E-01	6.32E 00	6.78E-01
180.10	4.0	2.08E-01	4.34E 00	9.33E-01
187.05	4.1	1.78E-01	3.16E 00	1.30E 00
194.65	4.3	1.44E-01	2.08E 00	2.06E 00
201.21	4.2	1.16E-01	1.33E 00	3.18E 00
207.55	4.1	8.77E-02	7.68E-01	5.39E 00
214.37	4.3	5.77E-02	3.33E-01	1.29E 01
218.09	4.0	4.13E-02	1.71E-01	2.37E 01
219.93	3.9	3.32E-02	1.10E-01	3.54E 01
221.87	3.9	2.47E-02	6.10E-02	6.40E 01
224.01	4.0	1.53E-02	2.34E-02	1.73E 02
226.21	4.0	5.63E-03	3.17E-03	1.28E 03
226.52	4.3	4.26E-03	1.82E-03	2.36E 03
227.17	4.0	1.41E-03	1.98E-04	2.05E 04
227.40	4.0	3.96E-04	1.57E-05	2.59E 05

Figure 3.10

Plot of logarithm (base e) of FWHM($\ell n\Gamma$) of the vibrational Raman spectrum of liquid CF_4 against the logarithm of the reduced temperature, ($\ell n\varepsilon$), $\varepsilon = [|T - T_c|/T_c]$.

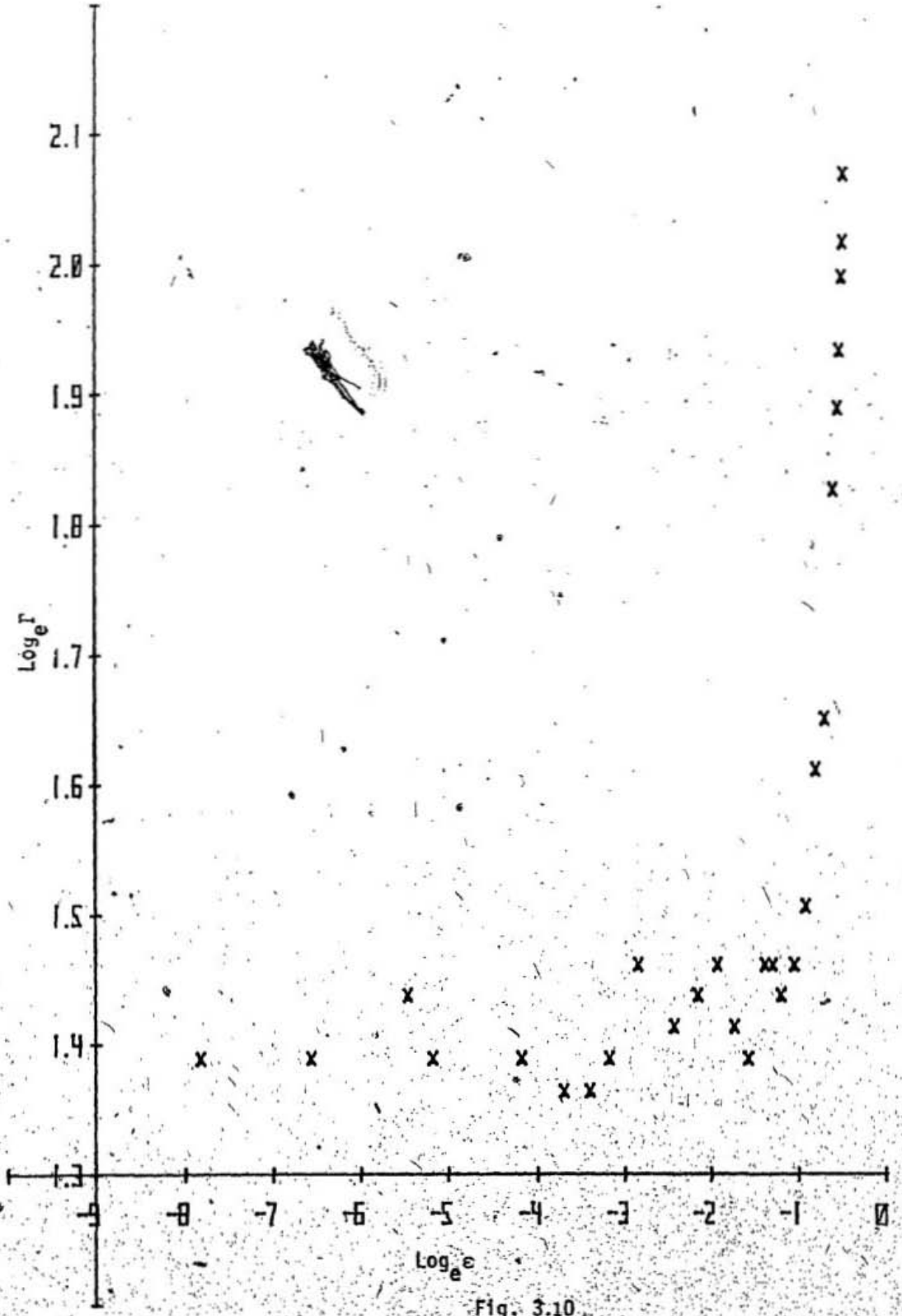

Fig. 3.10

hence Eq. (3.9) can not be used. Hills and Madden (1979) have predicted that in the region, $\omega \phi^{-1} \sim 1$, the curve ($\ell n \Gamma$ vs $\ell n \varepsilon$) should have a smooth turn. From Fig. 3.10 we find that in this region (see Table 3.7) the curve does have a smooth turn. The condition $\omega << \phi$ and $\omega \to 0$ arises below the boiling point. This region is very far away from the critical point, hence the critical exponent equation can not be supposed to be valid.

In the region $\log_e \varepsilon < -2.5$, as was shown in the case of methane, the Kawasaki (1970) correction is applicable and the critical exponent, as obtained in the last section, is $(-\frac{4}{3}\gamma + \frac{7}{3}\nu + a/3)$. No experimental values are available for any of these critical exponents for CF_4. Therefore the values obtained by Chang et al. (1979) for γ and ν are supposed to be applicable in the case of CF_4 i.e. $\gamma = 1.235$, $\nu = 0.625$ and $a = 0.53$ (Swinney & Cummins, 1968). On using these values one obtains $-\frac{4}{3}\gamma + \frac{7}{3}\nu + \frac{a}{3} = 0.011 \sim 0$. From Fig 3.10, one finds that in the region $\log_e \varepsilon < -2.5$, the slope of the line is zero. The reason for the increase in line width, in the case of O_2, N_2 and CH_4, is the increase in the amplitude and correlation length of the long wavelength density fluctuations as the critical point is approached. Howeven in case of CF_4 the contribution of long range or short range hydrodynamic fluctuations having wave vectors $Q < \kappa$ or $> \kappa$ appear to be absent. The reason for CF_4 behaving differently from CH_4 could be attributed to the C-F stretching mode. (The intensity of Raman scattered light, apart from other factors, also depends upon amplitude. The Raman intensity of the ν_1 mode of CF_4 is much smaller than that of the ν_1 mode of CH_4. The amplitude of the C-F mode in CF_4 is smaller by a factor of 6 than that of the C-H mode in CH_4.) The influence of anharmonicities for vibration

involving H atoms is large. If the amplitude is smaller and anharmonicities are also small, the motion will remain simple harmonic for a longer time (Herzberg, 1968). Because of the smaller amplitude in the C-F mode of vibration the effect of anharmonicities would be small. Oxtoby (1979) has shown that for simple harmonic motion the dephasing time is very high (i.e. the line would be narrow). If anharmonicities are taken into account the dephasing time is considerably reduced. If the vibration of the C-H mode is much more anharmonic than the C-F mode then it can be said that dephasing would be small in case of the C-F mode.

As the critical point is approached, the Raman vibrational line width becomes asymmetric. Hills and Madden (1979) have pointed out that close to the critical point, the fast motion condition is no longer applicable and it reaches the statistical or 'rigid-lattice limit, ($\Delta\tau_c >> 1$), (Kubo 1962). They obtained an expression for the half width at half height Δ as:

$$\Delta^2 = (2\pi^2)^{-1} \rho_e \Sigma_L B_L \int_0^\infty dQ\, Q^2\, S(Q)\, V_L^2 Q \qquad (3.14)$$

where B_L is the proportionality constant. Using the Ornstein-Zernicke expression for S(Q):

$$S(Q) = \frac{K_T}{(K_T)_o} \left(\frac{\kappa^2}{Q^2 + \kappa^2}\right) \qquad (3.15)$$

they obtain

$$\Delta^2 = J.\ \rho_e \frac{K_T}{(K_T)_o} \cdot \kappa^2 \qquad (3.16)$$

where J is a proportionality constant. It is seen that near the critical point Δ is proportional to $[(K_T/(K_{IT})_0)\ \kappa^{2}]^{1/2}$. This has a critical exponent of $(-\gamma + 2\nu)$. Using the values for γ and ν obtained by Chang et al., (1979) one finds that it has a value of zero. Hence theoretically it is seen that near the critical point the slope of the curve ($\ell n\Gamma$ vs $\ell n\varepsilon$) should be zero. Experimentally, one finds that the slope is zero. Thus we see that the observed constancy in line width is explained. It may be remarked that the equation (3.16) holds when $Q < \kappa$; even then it explains the phenomena. For more rigorous calculations the Kawasaki (1970) expression for S(Q) should be used.

REFERENCES

Ahmad S. F., 1977, Master's thesis, M.U.N., St. John's, Newfoundland.

Alekseyev V. and I. I. Sobelman, 1969, Sov. Phys. JETP, 28, 991.

Ali N., 1978, Master's thesis, M.U.N., St. John's, Newfoundland.

Bhatnagar S. S., E. J. Allin and H. L. Welsh, 1967, Can. J. Phys., 40, 9.

Bratos S. and E. Marechal, 1971, Phys. Rev., A3, 1078.

Brueck S. R. J., 1977, Chem. Phys. Letts., 50, 516.

Chang R. F., H. Burstyn and J. V. Sengers, 1979, Phys. Rev., A19, 866.

Clark J. H. R., in Advances in Infrared and Raman Spectroscopy (R. J. Clark and R. E. Hester Edts.), Heyden, London, 1978.

Clements W. R. L., 1972, Ph.D. Thesis, University of Toronto, Toronto

Clouter M. J., H. Kiefte and I. E. Morgan, 1975, Can. J. Phys., 53, 1727.

Clouter M. J. and H. Kiefte, 1977, J. Chem. Phys., 66, 1736.

*Clouter et al. (1979). To be Published.

Crawford R. K., W. B. Daniels and V. M. Cheng, 1975, Phys. Rev., 12, 1690.

Fisher M. E., 1964, J. Math. Phys., 5, 944.

Fischer S. F. and A. Laubereau, 1975, Chem. Phys. Letts., 35, 6.

Gammon P., 1978, Master's Thesis, M.U.N. St. John's, Newfoundland.

Goodwin R. D., 1974, N.B.S. Tech. Note No. 653.

Gordon R. G., 1965, J. Chem. Phys., 43, 1307.

Gray C. G. and J. Vankranedonk, 1966, Can. J. Phys., 44, 241.

Guggenheim E. A., 1945, J. Chem. Phys., 13, 253.

REFERENCES CONT'D

Herzberg G., 1968, Mol. Spectra and Mol. Structure II, (VanNostrand, Princeton).

Hills B. P., 1978 a, Mole. Phys., 35, 793.

Hills B. P., 1978 b, Mole. Phys., 35, 1471.

Hills B. P., 1979, Mole. Phys., 37, 949.

Hills B. P. and P. A. Madden, 1978, Mole. Phys. 35, 807.

Hills B. P. and P. A. Madden, 1979, Mole. Phys. 37, 937.

Jansoone V., H. Gielen, J. Deboelpaep and O.B. Verbake, 1970, Physica, 46, 213.

Jenkins F. A. and H. E. White, 1957, Fundamentals of Optics (McGraw Hill, New York).

Jones W. J., 1972, Contemp. Phys. 13, 419.

Kawasaki K., 1970, Ann. Phys. 61, 1.

Krynicki K., J. G. Powles and A. Rigamonti, 1977, Mole. Phys., 6, 1717.

Kubo R., in 'Fluctuation, Relaxation and Resonance in Magnetic Systems', 1961, Edited by D. Ter Harr (Oliver and Boyd, Edinburgh).

Landolt Bornstein, Zahlenwerte and Funktionen aus Physik - Chemie - Astronomie - Geophysik - Technik, Vol. 4, (Springer, Berlin).

Laubereau A., D. VonderLinde and W. Kaiser, 1972, Phys. Rev. Letts, 28, 1162.

Laubereau A., L. Krischner and W. Kaiser, 1973, Opt. Commun. 11, 74.

Laubereau A. and W. Kaiser, 1978, Rev. Mod. Phys., 50, 607.

REFERENCES CONT'D

May A. D., G. Varghese, J. C. Stryland and H. L. Welsh, 1964, Can. J. Phys. 42, 1058.

Morgan I. E., 1976, Master's Thesis, M.U.N. St. John's, Newfoundland.

Nafie L. A. and W. L. Peticolas, 1972, J. Chem. Phys., 57, 3145.

Oxtoby D. W. (1979), Adv. Chem. Phys. (To be published).

Rothschild W. G., 1976, J. Chem. Phys., 65, 2958.

Schroeder J., V. H. Schiemann and J. Jones, 1977, Mole. Phys. 34, 1501.

Stanley E., 1971, 'Introduction to Phase Transitions and Critical Phenomena' (Clarendon Press, Oxford).

Swinney H. L. and H. Z. Cummins, 1968, Phys. Rev. 171, 152.

Temkin S. I and A. I. Burshtein, 1976, JETP Letts., 24, 2.

Varghese G., 1967, Ph.D. Thesis, University of Toronto, Toronto.

Weber A., in 'The Raman Effect Vol. 2. (A. Anderson Ed.), Marcel Dekker, New York, 1973.